Mathematical Biosciences and Engineering

http://www.aimspress.com/journal/mbe

MBE, 20(8): 15167–15200.
DOI: 10.3934/mbe.2023679
Received: 06 April 2023
Revised: 17 June 2023
Accepted: 26 June 2023
Published: 18 July 2023

Research article

Mathematical modelling of the interactive dynamics of wild and *Microsporidia MB*-infected mosquitoes

Charlène N. T. Mfangnia[1,2], Henri E. Z. Tonnang[2,*], Berge Tsanou[1,3] and Jeremy Herren[2]

[1] Department of Mathematics and Computer Science, Faculty of Science, University of Dschang, P.O. Box: 67, Cameroon

[2] International Centre of Insect Physiology and Ecology (*icipe*), Nairobi, P.O. Box: 30772, Kenya

[3] Department of Mathematics and Applied Mathematics, University of Pretoria, Pretoria 0002, South Africa

* **Correspondence:** Email: htonnang@icipe.org.

Abstract: A recent discovery highlighted that mosquitoes infected with *Microsporidia MB* are unable to transmit the *Plasmodium* to humans. *Microsporidia MB* is a symbiont transmitted vertically and horizontally in the mosquito population, and these transmission routes are known to favor the persistence of the parasite in the mosquito population. Despite the dual transmission, data from field experiments reveal a low prevalence of *MB*-infected mosquitoes in nature. This study proposes a compartmental model to understand the prevalence of *MB*-infected mosquitoes. The dynamic of the model is obtained through the computation of the basic reproduction number and the analysis of the stability of the MB-free and coexistence equilibria. The model shows that, in spite of the high vertical transmission efficiency of *Microsporidia MB*, there can still be a low prevalence of *MB*-infected mosquitoes. Numerical analysis of the model shows that male-to-female horizontal transmission contributes more than female-to-male horizontal transmission to the spread of MB-infected mosquitoes. Moreover, the female-to-male horizontal transmission contributes to the spread of the symbiont only if there are multiple mating occurrences for male mosquitoes. Furthermore, when fixing the efficiencies of vertical transmission, the parameters having the greater influence on the ratio of MB-positive to wild mosquitoes are identified. In addition, by assuming a similar impact of the temperature on wild and *MB*-infected mosquitoes, our model shows the seasonal fluctuation of *MB*-infected mosquitoes. This study serves as a reference for further studies, on the release strategies of MB-infected mosquitoes, to avoid overestimating the MB-infection spread.

Keywords: Microsporidia MB; Plasmodium transmission-blocking; vertical-horizontal transmission; compartmental modelling; seasonality; malaria bio-control

1. Introduction

Microsporidia is a significant genus of obligate intracellular parasites with a wide range of species that are currently assumed to be highly developed *fungi* [1]. These parasites can be found in a variety of animals, including mosquitoes [1]. We can cite for example *Anncaliia algerae*, *vavraia culicis*, *Parathelohania (aophelis, obesa)* and *Hazardia sp.* in *Anopheles mosquitoes*; *Hazardia milleri*, *culicosporella lunata*, *Amblyospora opacita* in *culex*; *Edharzardia aedis* in *Aedes aegypti* [1, 2] and, more recently, *Microsporidia MB* in *Anopheles arabiensis*, *funestus*, *gambiae* and *coluzzi* [3–5].

The transmission of the *Microsporidian* species in the insect population is driven by the vertical and horizontal transmission [6]. For some *Microsporidian* species, the transmission is exclusively vertical or exclusively horizontal while in other cases the transmission is mixed. For instance, *Edhazardia aedis* exhibits both horizontal and vertical transmissions [7]. The horizontal transmission of *Edhazardia aedis* occurs when a spore is ingested by the mosquito larva. During the maturation process, the spore will spread all over the mosquito body and in case the adult mosquito is a female, the ovaries and oocystes will be infected. The infection is then passed to the offspring (vertical transmission).

Microsporidia MB is another type of parasite that is spreading both vertically and horizontally [3,4]. Its singularity is that the horizontal transmission is not occurring at the larvae stage, but between adult mosquitoes (male to female or female to male) through mating, with a higher transmission efficiency from male to female rather than from female to male (56% on average compared to 33%) [3, 4]. *Microsporidian* species, such as *Microsporidia MB*, that rely mostly on sexual horizontal transmission, have a higher level of host specificity. This could explain why this symbiont has yet to be discovered in a non-anopheline host.

In most cases of host-parasite interaction, the parasite causes damage and mortality to the host, thus inducing a fitness cost to its mosquito host. In contrast, the host reacts by lowering the parasite's negative effects and the infection success probability [8]. However, *Microsporidia MB* does not significantly affect the host's fertility or survival, and its presence is advantageous since it blocks the transmission of the *Plasmodium* [4]. As a result, disseminating this symbiont throughout the population of malaria vectors could be a promising strategy to stop the spread of malaria. Although there are currently no field trials, some analysis of the dynamics of transmission of the *Microsporidia MB* is necessary to assess the feasibility of this potential intervention and guide field experiments. It is worth noting that understanding the dynamics of symbiont transmission as well as the effects on the incidence of malaria is essential before considering potential strategies to replace the mosquito population with the *MB*-infected mosquito population as done for other endosymbionts like Wolbachia [9].

Several mathematical models with vertical and/or horizontal transmission have been developed previously for a few symbiont-based mosquito control strategies. The study conducted by Lipsitch et al. [10], is among the pioneer research focusing on assessing the role of vertical and horizontal transmission in maintaining infection in a host population. This study highlighted the necessity of both vertical and horizontal transmission to achieve and stably maintain a 100% infection prevalence. In the recent past, a number of mathematical models have been developed to mimic the introduction of *Wolbachia* (a maternally transmitted symbiont that is unable to transmit the dengue virus) into populations of *Aedes aegypti* [11–15]. Several models, such as [9], [16], and [17] aim to design optimal release strategies to increase *Wolbachia* prevalence in nature. *Wolbachia*'s success in reducing dengue has been shown in regions such as Northern Queensland in Indonesia [18]. In addition, *Wolbachia* was identi-

fied to be naturally present in the anopheles mosquito population, and a mathematical model [19] was developed to assess the feasibility in malaria vector bio-control. However, almost no model focused on analysing the dynamics of the spread of *Microsporidia MB* in the wild mosquito population [3]. The dynamics of the spread of *Microsporidia MB* differs from the dynamics of the spread of *Wolbachia* because of the difference in their respective features. Cytoplasmic incompatibility (CI) [20] that makes a wild *Aedes Aegypti* female to lay non-viable eggs after mating with a *Wolbachia*-infected male, and is affecting many *Wolbachia* strains is not a characteristic of *Microsporidia MB*. In contrast, *Microsporidia MB*-infected males infect wild females through horizontal transmission and infection reaches the new generation through vertical transmission. Therefore, this study proposes a deterministic model to analyze the dynamics of the spread of *MB*-infected mosquitoes, to understand and explain the low prevalence of the *Microsporidia MB* in the mosquito population as reported by [3, 4], to identify the factors driving the spread of *MB*-infected mosquitoes and to describe the seasonal variation of the prevalence of *MB*-infected mosquitoes.

The following is the structure of this paper: Section 2 describes how the model was formulated based on the mosquito life-cycle characteristics. Section 3 highlights the thresholds for the existence or persistence of the mosquito populations. Section 4 presents the equilibria and their stability along with the interpretation of the findings. The proof of the analytical results is provided in Section 5. Section 6 discusses and concludes.

2. Model formulation

This section describes the various assumptions that are considered alongside the formulation of the model. The mosquito undergoes several stages for its development and maturation which are eggs, larvae, pupae and adults [21]. However, to reduce the complexity of the model, this model considers only two stages of mosquito development which are the egg stage $\mathcal{E}$ and the adult stage. The adult stage is divided into the male population M_T and the female population F_T. As our interest is to study the interaction of wild and *MB*-infected mosquitoes, the male population is divided into wild males M_n and *MB*-positive males M_p. Similarly, the female population is divided into wild females (unfertile) F_n, the pregnant wild females F_n^m, *MB*-positive females (unfertile) F_p and the pregnant *MB*-positive females F_p^m. Thus, $M_T = M_p + M_n$ and $F_T = F_p + F_n + F_p^m + F_n^m$.

The lab experiments reported that the transmission of *Microsporidia MB* in the mosquito population is driven by horizontal transmission and vertical transmission [3, 4], which we have to consider to estimate the new *MB*-infected mosquitoes either females F_p or males M_p. The vertical transmission describes the transmission of the symbiont from the mother to the eggs and is accounted for in the model by considering that the fraction β_v of the progeny of MB-positive pregnant females will join the class of *MB*-infected eggs $\mathcal{E}_p$, while the remaining fraction $(1 - \beta_v)$ join the class of wild eggs $\mathcal{E}_n$. In the previous statement, β_v represents the efficiency of vertical transmission. With this formulation, we consider both imperfect vertical transmission which happens when $\beta_v < 1$ and the perfect vertical transmission which happens when $\beta_v = 1$. On the other hand, horizontal transmission describes the transmission from one adult partner to another one during mating and is conditioned on the female side by a unique mating possibility [22]. Figure 1 presents a summary flowchart diagram displaying the transmission process of the symbiont and its evolution within the different subgroups of the mosquito population.

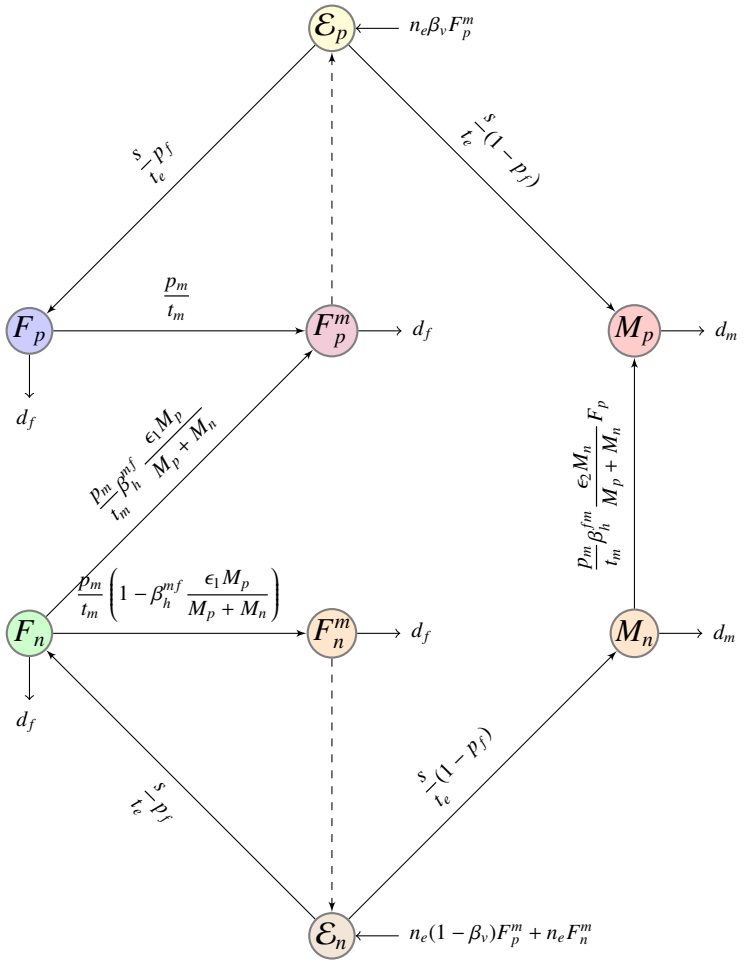

Figure 1. Flowchart describing the transmission process of the symbiont and its evolution within the different subgroups of the mosquito population.

The transmission process and the resulting equations are described in the following manner. A newly emerged female mosquito (F_p or F_n) mates and join the class of pregnant females (F_p^m or F_n^m). After mating and blood-feeding, the pregnant females lay new eggs and the number of eggs per female per unit of time is designed by n_e. While defining the number of eggs produced by a female mosquito, we are considering the impact of the availability of resources by including the carrying capacity. The carrying capacity represents the maximum number of eggs that can be sustained in a given area depending on the environmental resources. Thus, the new progeny is included in the model as $n_e\,(1-\mathcal{E}/K)$. For the status of the eggs, whether there will be the presence or not of the symbiont, it is assumed according to prior studies [3,4] that eggs from negative females F_n^m will always be negative, while eggs from positive female F_p^m can be positive depending on the efficiency of vertical transmission β_v. In fact, the vertical transmission describes the transmission of the symbiont from the mother to the eggs and is accounted for in the model by considering that the fraction β_v of the progeny will join the class of *MB*-infected eggs $\mathcal{E}_p$ while the remaining fraction $(1-\beta_v)$ join the class of wild eggs $\mathcal{E}_n$. Then, eggs ($\mathcal{E}_p$ or $\mathcal{E}_n$) mature as *MB*-positive adults (F_p and M_p) or wild adults (F_n and M_n) respectively. With this assertion, we are assuming that an MB-infected egg or mosquito cannot lose the infection and will keep it during its lifespan. The maturation time is defined based on the egg development time t_e and the

proportion of eggs that will reach the adult stage depends on the survival rate s. Thus, a fraction (s/t_e) of eggs ($\mathcal{E}_p$ or $\mathcal{E}_n$) leave the compartment of eggs to join the compartment adults females ((F_p and M_p) or (F_n and M_n), respectively). Therefore, the rates of variation of the mosquito egg populations $\mathcal{E}_p$ and $\mathcal{E}_n$ are given by:

$$\frac{d\mathcal{E}_p}{dt} = n_e\beta_v F_p^m\left(1-\frac{\mathcal{E}}{K}\right) - \frac{s}{t_e}\mathcal{E}_p; \text{ and } \frac{d\mathcal{E}_n}{dt} = n_e F_n^m\left(1-\frac{\mathcal{E}}{K}\right) + n_e(1-\beta_v)F_p^m\left(1-\frac{\mathcal{E}}{K}\right) - \frac{s}{t_e}\mathcal{E}_n.$$

Newly emerged adults can either be females or males. To consider this distinction, we define the proportion p_f of females among new adults as the sex ratio of emerging adults. A proportion p_f of eggs emerges as females while the remaining $(1-p_f)$ emerges as males. Thus, the population of females (F_p or F_n) is increased by the newly emerged females at a rate (sp_f/t_e). A few days after emerging as an adult (t_m), a proportion p_m of females (F_p or F_n) mate with males generally during swarming [23]. To consider a unique mating possibility for the females, the model distinguished the compartment of pregnant females (F_p^m and F_n^m) for female mosquitoes that have already mated. Thus, a proportion (p_m/t_m) leaves the compartments (F_p or F_n) and enters the compartment of pregnant females as wild F_n^m or as MB-positive F_p^m depending on their initial status and the effectiveness of horizontal transmission. In addition, by considering the female mosquito death rate d_f, the rates of variation of the non-pregnant female populations F_p and F_n are given by:

$$\frac{dF_p}{dt} = \frac{sp_f}{t_e}\mathcal{E}_p - d_f F_p - \frac{p_m}{t_m}F_p; \text{ and } \frac{dF_n}{dt} = \frac{sp_f}{t_e}\mathcal{E}_n - d_f F_n - \frac{p_m}{t_m}F_n.$$

As reported from lab experiment [3, 4], the symbiont MB can be transmitted horizontally during the mating process from one partner to another one. A female can mate either with a male positive to the symbiont M_p or a male negative to the symbiont M_n. The success of the horizontal transmission depends on the *MB* status of the male partner and the male-to-female horizontal transmission probability β_h^{mf}. We choose to define the probability of mating with an *MB*-positive male by $\epsilon_1 M_p/M_T$, where ϵ_1 is the attractiveness of *MB*-positive males compared to wild males. Thus, the transmission probability success of the symbiont from an *MB*-positive male to a wild female is expressed as $\beta_h^{mf}\epsilon_1 M_p/M_T$. MB-positive females automatically join the class F_p^m after mating, whereas *MB*-negative females can join the class F_p^m if they have acquired the infection or join the class F_n^m if they are still uninfected. Thus, the fraction $(p_m/t_m)(\beta_h^{mf}\epsilon_1 M_p/M_T)F_n$ joins the class F_p^m while the fraction $(p_m/t_m)(1-\beta_h^{mf}\epsilon_1 M_p/M_T)F_n$ joins the class F_n^m. In addition, by considering the female mosquito death rate d_f, the rates of variation of the pregnant female populations F_p^m and F_n^m are given by :

$$\frac{dF_p^m}{dt} = \frac{p_m}{t_m}F_p + \frac{p_m}{t_m}\beta_h^{mf}\frac{\epsilon_1 M_p}{M_p+M_n}F_n - d_f F_p^m; \text{ and } \frac{dF_n^m}{dt} = \frac{p_m}{t_m}F_n - \frac{p_m}{t_m}\beta_h^{mf}\frac{\epsilon_1 M_p}{M_p+M_n}F_n - d_f F_n^m.$$

In the same way, negative males M_n who mate with females F_p can become positive depending on the horizontal transmission efficiency from female to male β_h^{fm} and the attractiveness of wild males to MB-positive females. To define the new *MB*-positive males that join the class M_p after mating, we stand from the point of view that the female is the one choosing the male partner [24], and we use the conservation contact to assert that the number of new infected *MB*-positive males at time t is equal to the number of *MB*-positive females that have successfully mated and transmitted the symbiont to

a susceptible male partner. The mentioned transmission probability success of the symbiont from an *MB*-positive female to a wild male depends on the female-to-male horizontal transmission probability β_h^{fm} and is expressed as $\beta_h^{fm}\epsilon_2 M_n/M_T$, where ϵ_2 is the attractiveness of wild males compared to *MB*-positive males. As explained above, the population of males (M_p or M_n) is increased by the newly emerged males at a rate $(s(1-p_f)/t_e)$. In addition, by considering the male mosquito death rate d_m, the rates of variation of the male populations M_p and M_n are given by :

$$\frac{dM_p}{dt} = \frac{s(1-p_f)}{t_e}\mathcal{E}_p + \frac{p_m}{t_m}\beta_h^{fm}\frac{\epsilon_2 M_n}{M_p+M_n}F_p - d_m M_p; \text{ and } \frac{dM_n}{dt} = \frac{s(1-p_f)}{t_e}\mathcal{E}_n - \frac{p_m}{t_m}\beta_h^{fm}\frac{\epsilon_2 M_n}{M_p+M_n}F_p - d_m M_n.$$

Remark. *The dimensionless parameters ϵ_1 and ϵ_2 are defined to guarantee that the quantities $\epsilon_1(M_p/M_T)$, and $\epsilon_2(M_n/M_T)$ remains between* 0 *and* 1*, as they designate probability values.*

Table 1 gathers all the parameters used in the model and the transmission mechanism is described by the equations in System (2.1).

$$\begin{cases} \dfrac{d\mathcal{E}_p}{dt} &= n_e\beta_v F_p^m\left(1-\dfrac{\mathcal{E}}{K}\right) - \dfrac{s}{t_e}\mathcal{E}_p; \\ \dfrac{dF_p}{dt} &= \dfrac{sp_f}{t_e}\mathcal{E}_p d_f F_p - \dfrac{p_m}{t_m}F_p; \\ \dfrac{dF_p^m}{dt} &= \dfrac{p_m}{t_m}F_p + \dfrac{p_m}{t_m}\beta_h^{mf}\dfrac{\epsilon_1 M_p}{M_p+M_n}F_n - d_f F_p^m; \\ \dfrac{dM_p}{dt} &= \dfrac{s(1-p_f)}{t_e}\mathcal{E}_p + \dfrac{p_m}{t_m}\beta_h^{fm}\dfrac{\epsilon_2 M_n}{M_p+M_n}F_p - d_m M_p; \\ \dfrac{d\mathcal{E}_n}{dt} &= n_e F_n^m\left(1-\dfrac{\mathcal{E}}{K}\right) + n_e(1-\beta_v)F_p^m\left(1-\dfrac{\mathcal{E}}{K}\right) - \dfrac{s}{t_e}\mathcal{E}_n; \\ \dfrac{dF_n}{dt} &= \dfrac{sp_f}{t_e}\mathcal{E}_n - d_f F_n - \dfrac{p_m}{t_m}F_n; \\ \dfrac{dF_n^m}{dt} &= \dfrac{p_m}{t_m}F_n - \dfrac{p_m}{t_m}\beta_h^{mf}\dfrac{\epsilon_1 M_p}{M_p+M_n}F_n - d_f F_n^m; \\ \dfrac{dM_n}{dt} &= \dfrac{s(1-p_f)}{t_e}\mathcal{E}_n - \dfrac{p_m}{t_m}\beta_h^{fm}\dfrac{\epsilon_2 M_n}{M_p+M_n}F_p - d_m M_n. \end{cases} \tag{2.1}$$

In the next section, we are highlighting two important thresholds for the evolution of the population whose dynamics are described by the System (2.1) : R_1 the average number of new female adults produced by a wild female during its lifetime and $R_0^{(TV)}$ the ratio of new adult MB-infected females produced by an MB-infected female during its lifetime to R_1.

Table 1. Parameters of the malaria model (**N**: Notation).

N	Definition	Value [Range]	Source
β_h^{fm}	Efficiency of horizontal transmission from female to male.	0.33	[3]
β_h^{mf}	Efficiency of horizontal transmission from male to female.	0.56	[3]
t_m	average time for mating	3 (day)	[25]
p_m	Proportion of females that mate	0.7665 [0.533–1]	[25]
ϵ_1	Attractiveness of *MB*-positive males compared to wild males	variable	-
ϵ_2	Attractiveness of wild males compared to *MB*-positive males	variable	-
β_v	Efficiency of vertical transmission	0.45 [0.45–1]	[4]
t_e	Average development time from egg to adult	19.35 [0–31] (day)	[26]
n_e	Fecundity (number of eggs per female per day)	1 [0.8–6]	[27]
s	Survival from egg to adult	0.72 [0–0.72]	[4]
p_f	Proportion of females	0.5	[28]
d_f	Female death rate	0.0345 (1/day)	[29]
K	Carrying capacity	Variable	Assumed

3. Preliminary results

The basic offspring number for the entire mosquito population is obtained through the computation of the equilibria (presented above) and defined as :

$$R_1 = \frac{n_e p_m p_f}{d_f \left(t_m d_f + p_m\right)}. \tag{3.1}$$

From the entomological perspective, the defined number R_1 represents the average number of new female adult mosquitoes produced by an adult female mosquito introduced within a population of only male mosquitoes during its entire life cycle. In the expression of R_1, $p_m/(t_m d_f + p_m)$ is the probability that an adult female survives the mating process; $n_e.p_f.(1/d_f)$ is the number of female eggs produced, by a female that has mated, during its lifetime period. Thus, having $R_1 > 1$ ensures the persistence of the entire mosquito population.

In this context, the basic reproduction number [30] describes the average number of secondary *MB*-infected mosquitoes caused by the introduction of an *MB*-infected mosquito in a population of wild mosquitoes. The transmission of *Microsporidia MB* occurs both horizontally and vertically and new infected both vertically and horizontally are considered for the computation of the basic reproduction number. However, because the mosquito lifespan is short (on average 22 days for males and 32 days for females [29]), Microsporidia infection can be maintained in the mosquito population only if new horizontally *MB*-infected mosquitoes are able to transmit the symbiont vertically. Thus, instead of computing the basic reproduction number, we target only the new infected vertically and the corresponding target reproduction number $\mathcal{R}_0^{(TV)}$ determines the establishment of the *Microsporidia MB* in

the mosquito population. $\mathcal{R}_0^{(TV)}$ is computed using the method described in [31] and is defined as :

$$\mathcal{R}_0^{(TV)} = \beta_v \left(1 + \epsilon_1 \beta_h^{mf} + \frac{\epsilon_1 \beta_h^{mf} \epsilon_2 \beta_h^{fm} p_m p_f}{(1 - p_f)\left(t_m d_f + p_m\right)} \right) = \Gamma_1 + \Gamma_2 + \Gamma_3; \tag{3.2}$$

where,

$$\Gamma_1 = \beta_v; \;\; \Gamma_2 = \beta_v \epsilon_1 \beta_h^{mf} \text{ and } \Gamma_3 = \frac{\epsilon_1 \beta_h^{mf} \epsilon_2 \beta_h^{fm} p_m p_f}{(1 - p_f)\left(t_m d_f + p_m\right)}.$$

The proof of the computation of the target reproduction number is given in Section 5.1. We deduce from the definition of $\mathcal{R}_0^{(TV)}$ that there are three ways in which the actual population of *MB*-positive mosquitoes contributes to the new *MB*-infected mosquitoes for the next generation:

- The progeny of females already *MB*-positive at birth and the probability of transmission is given by $\Gamma_1 = \beta_v$;
- The progeny of females that will acquire the symbiont after mating and the probability of transmission is given by Γ_2;
- The progeny of females *MB*-infected through mating, by males *MB*-positive that have been previously infected by females already *MB*-positive at births and have survived for a new mating and the probability of transmission is given by Γ_3.

Hence, $R_1 \mathcal{R}_0^{(TV)}$ is the average number of new female progeny produced by a single MB-infected female mosquito through the transmission (horizontal, vertical and combination of both), during its entire lifespan when introduced in a population of wild mosquitoes. As a result, $\mathcal{R}_0^{(TV)}$ represents the ratio of the new MB-infected female progeny of an MB-infected female to the wild female progeny of a wild female mosquito. Thus, with $\mathcal{R}_0^{(TV)} > 1$, the prevalence of MB-infected mosquitoes tends to increase and the MB-infected mosquito population persists. This threshold for the persistence of MB-infected mosquitoes corroborates with the spread conditions for horizontally and vertically transmitted parasites given by Lipsitch et al. [10]. Besides, we observe from the definition of our target reproduction number, that the impact of the female-to-male horizontal transmission depends both on the multiple mating occurrences for males and on the efficiency of the male-to-female horizontal transmission.

In the next section, we prove the mathematical and ecological well-posedness of the formulated model. In addition, we carry out the mathematical analysis of the autonomous model (2.1) to predict the long-term behaviour of the dynamic of transmission of *Microsporidia MB* inside the wild mosquito population. Moreover, we highlight the requirements that must be met in order to explore the following scenarios: extinction of the entire mosquito population, extinction of *MB*-positive mosquitoes, the coexistence of *MB*-positive and wild mosquitoes and complete infection by the symbiont (i.e, population replacement, where wild mosquitoes become MB-infected).

4. Main results and interpretation

We start by proving that model (2.1) is well posed from the mathematical and ecological point of view. This is ensuring that the model admits a unique positive solution defined for all time t.

Theorem 1. *For positive initial conditions, the solution of the Cauchy problem associated with system* (2.1) *is unique, positive and bounded on its existence interval. Let*

$$X = (F_p, F_n, F_p^m, F_n^m, \mathcal{E}_p, \mathcal{E}_n, M_p, M_n);$$

be the unique solution of the associated Cauchy problem, then X is defined for all time, and lies with its initial condition in the following set.

$$\Delta = \left\{ \begin{pmatrix} F_p \\ F_n \\ F_p^m \\ F_n^m \\ \mathcal{E}_p \\ \mathcal{E}_n \\ M_p \\ M_n \end{pmatrix} \in \mathbb{R}_+^8 \;\middle|\; \begin{pmatrix} 0 \le \mathcal{E} \le K \\ 0 \le F \le \dfrac{t_m s p_f K}{t_e\left(t_m d_f + p_m\right)} \\ 0 \le F^m \le \dfrac{p_m s p_f K}{d_f t_e\left(t_m d_f + p_m\right)} \\ 0 \le M \le \dfrac{s(1-p_f)}{t_e d_m} K \end{pmatrix} \right\}$$

where $F = F_p + F_n$, $F^m = F_p^m + F_n^m$, $\mathcal{E} = \mathcal{E}_p + \mathcal{E}_n$ *and* $M = M_p + M_n$.

Theorem 1 shows that all the mosquito population starts and remains in the bounded set Δ and the proof is presented in Section 5.2. Then, we proceed with the determination of the equilibria and the study of their stability in order to assess the long-term behaviour of the system. The number of equilibria depends on whether the vertical transmission is imperfect ($\beta_v < 1$) or perfect ($\beta_v = 1$) and is determined accordingly. We have identified four equilibria which are listed below with the corresponding existence conditions. The details in the computation process are presented in Section 5.3. The equilibria of system (2.1) include :

- The trivial steady state, corresponding to the situation where there is no mosquito in the population, always exists and is defined by

$$ZE = (0, 0, 0, 0, 0, 0, 0, 0).$$

- The *MB*-free equilibrium is associated with the scenario where all the *MB*-infected mosquitoes are absent in the population and exists if and only if $R_1 > 1$. It is obtained from system (2.1) by replacing $F_p = 0$, $F_p^m = 0$, $\mathcal{E}_p = 0$, and $M_p = 0$. Then, the *MB*-free equilibrium denoted by MFE is :

$$MFE = X^* = (0,\ 0,\ 0,\ 0,\ \mathcal{E}_n^*,\ F_n^*,\ F_n^{m^*},\ M_n^*);$$

where,

$$\begin{cases} F_n^* = \dfrac{t_m s p_f}{t_e\left(t_m d_f + p_m\right)} \mathcal{E}_n^*; & M_n^* = \dfrac{s(1-p_f)}{t_e d_m} \mathcal{E}_n^*; \\ F_n^{m^*} = \dfrac{p_m s p_f}{d_f t_e\left(t_m d_f + p_m\right)} \mathcal{E}_n^*; & \mathcal{E}_n^* = K\left(1 - \dfrac{1}{R_1}\right). \end{cases} \tag{4.1}$$

- The coexistence equilibrium corresponds to the situation where *MB*-positive and *MB*-negative mosquitoes co-evolve and exists if and only if $\beta_v < 1$, $R_1 > 1$ and $\mathcal{R}_0^{(TV)} > 1$. This steady state is denoted by :

$$CE = \overline{X} = (\overline{\mathcal{E}_p},\ \overline{F_p},\ \overline{F_p^m},\ \overline{M_p},\ \overline{\mathcal{E}_n},\ \overline{F_n},\ \overline{F_n^m},\ \overline{M_n});$$

where,

$$\begin{cases} \overline{F_p} = t_m A \overline{\mathcal{E}_p}; & \overline{F_n} = t_m A \overline{\mathcal{E}_n}; \\ \overline{F_p^m} = \dfrac{p_m A}{\beta_v d_f} \overline{\mathcal{E}_p}; & \overline{F_n^m} = \dfrac{p_m A}{d_f} \left[\overline{\mathcal{E}_n} + \left(1 - \dfrac{1}{\beta_v}\right) \overline{\mathcal{E}_p} \right]; \\ \overline{M_p} = C \left(\dfrac{s(1-p_f)(1-\beta_v)}{\epsilon_1 \beta_h^{mf} \beta_v t_e d_m} \right) \dfrac{\overline{\mathcal{E}_p}}{\overline{\mathcal{E}_n}}; & \overline{M_n} = C \left(\dfrac{s(1-p_f)}{t_e d_m} \right) - \overline{M_p}; \\ \overline{\mathcal{E}_p} = C \left(\dfrac{-1 + R_0^{(TV)}}{B(1-\beta_v) + \epsilon_1 \beta_v \beta_h^{mf} (1+B)} \right); & \overline{\mathcal{E}_n} = C - \overline{\mathcal{E}_p}. \end{cases} \tag{4.2}$$

with $A = \dfrac{s p_f}{t_e \left(t_m d_f + p_m\right)} \overline{\mathcal{E}_p}$; $B = \dfrac{p_m p_f \epsilon_2 \beta_h^{fm}}{(1-p_f)\left(t_m d_f + p_m\right)}$, $C = K\left(1 - \dfrac{1}{R_1}\right)$ and $\mathcal{R}_0^{(TV)}$ is the reproduction number of our model presented above.

- The complete-infection equilibrium corresponds to the situation where there are no wild mosquitoes and exists if and only if $\beta_v = 1$ and $R_1 < 1$. Thus, when the vertical transmission is perfect, the coexistence equilibrium is replaced by the complete-infection equilibrium *CIE*, and the symbiont can spread throughout the entire mosquito population. This the desired and ideal situation for the complete eradication of malaria if this equilibrium point is also proved to be locally (asymptotically) stable. The *CIE* is found by setting $F_n = F_n^m = \mathcal{E}_n = M_n = 0$ and the steady state is denoted by:

$$CIE = X^{**} = (\mathcal{E}_p^{**},\ F_p^{**},\ F_p^{m^{**}},\ M_p^{**},\ 0,\ 0,\ 0,\ 0);$$

where,

$$\begin{cases} F_p^{**} = \dfrac{t_m s p_f}{t_e \left(t_m d_f + p_m\right)} \mathcal{E}_p^{**}; & F_p^{m^{**}} = \dfrac{p_m s p_f}{d_f t_e \left(t_m d_f + p_m\right)} \mathcal{E}_p^{**}; \\ M_p^{**} = \dfrac{s(1-p_f)}{t_e d_m} \mathcal{E}_p^{**}; & \mathcal{E}_p^{**} = K\left(1 - \dfrac{1}{R_1}\right). \end{cases} \tag{4.3}$$

Once we have identified the equilibria of the system, the long-term behaviour is investigated by studying the stability properties of the equilibrium points. The local asymptotic stability of an equilibrium proves that if there is a small perturbation, the solution of the system will remain in a close neighbourhood and finally returns to the equilibrium state [32]. Theorem 2 resumes the local asymptotic stability properties of the equilibria and the proof is given in Section 5.4.

Theorem 2. *The following statements hold:*

1) The zero equilibrium ZE is locally asymptotically stable if $R_1 < 1$ *and unstable if* $R_1 > 1$.

2) The MB*-free equilibrium is locally asymptotically stable if* $R_1 > 1$ *and* $\mathcal{R}_0^{(TV)} < 1$ *and unstable if* $R_1 > 1$ *and* $\mathcal{R}_0^{(TV)} > 1$.

3) The coexistence equilibrium CE is locally asymptotically stable whenever it exists, meaning, $\beta_v < 1$, $R_1 > 1$ *and* $\mathcal{R}_0^{(TV)} > 1$.

4) The complete-infection equilibrium CIE exists and is locally asymptotically stable if $\beta_v = 1$ *and* $R_1 > 1$.

Concerning the global stability, Theorem 3 presents the established results and the proof is given in Section 5.5.

Theorem 3. *The following statements hold:*

1) The zero equilibrium ZE is globally asymptotically stable whenever $R_1 < 1$.

2) The unique non-zero equilibrium

$$(\mathcal{E}^*,\ F^*, F^{m*}, M^*) = \left(\mathcal{E}^*,\ \frac{p_m s p_f}{d_f t_e\left(t_m d_f + p_m\right)}\mathcal{E}^*,\ \frac{t_m s p_f}{t_e\left(t_m d_f + p_m\right)}\mathcal{E}^*,\ \frac{s(1-p_f)}{t_e d_m}\mathcal{E}^*\right);\ \ \mathcal{E}^* = K\left(1 - \frac{1}{R_1}\right); \tag{4.4}$$

is globally asymptotically stable whenever $R_1 > 1$ *for the system describing the evolution of the total egg population* $\mathcal{E} = \mathcal{E}_p + \mathcal{E}_n$*, the total female population* $F = F_p + F_n$ *and the total pregnant female population* $F^m = F_p^m + F_n^m$.

$$\begin{cases} \dfrac{d\mathcal{E}}{dt} = n_e F^m(1 - \dfrac{\mathcal{E}}{K}) - \dfrac{s}{t_e}\mathcal{E}; & \dfrac{dF^m}{dt} = \dfrac{p_m}{t_m}F - d_f F^m; \\ \dfrac{dF}{dt} = \dfrac{s}{t_e}p_f\mathcal{E} - (d_f + \dfrac{p_m}{t_m})F; & \dfrac{dM}{dt} = \dfrac{s}{t_e}(1-p_f)\mathcal{E} - d_m M. \end{cases} \tag{4.5}$$

It is important to note that when the vertical transmission is perfect ($\beta_v < 1$), $\mathcal{R}_0^{(TV)} > 1$ and the *MB*-free equilibrium is always unstable. Overall, the local asymptotic stability of the equilibria of the system (2.1) for both imperfect and perfect vertical transmission cases is resumed in Table 2.

Table 2. Stability of the equilibria. $\beta_v = 1$ represents the perfect vertical transmission case while $\beta_v < 1$ the case of imperfect vertical transmission.

	Equilibria	Existence	Local stability	Local instability
$\beta_v < 1$	ZE	always exists	$R_1 < 1$	$R_1 > 1$
	MFE	$R_1 > 1$	$R_1 > 1$ & $\mathcal{R}_0^{(TV)} < 1$	$R_1 > 1$ & $\mathcal{R}_0^{(TV)} > 1$
	CE	$R_1 > 1$ & $\mathcal{R}_0^{(TV)} > 1$	$R_1 > 1$ & $\mathcal{R}_0^{(TV)} > 1$	-
$\beta_v = 1$	ZE	always exists	$R_1 < 1$	$R_1 > 1$
	MFE	$R_1 > 1$	-	$R_1 > 1$
	CIE	$R_1 > 1$	$R_1 > 1$	-

Remark. *We deduce from the study of the local asymptotic stability of the equilibria of System* (2.1) *summarized in Table 2, that exhibits only trans-critical bifurcations. In fact, in the case of imperfect maternal transmission ($\beta_v < 1$), there is a forward bifurcation at $R_1 = 1$ where the ZE equilibrium changes from stable ($R_1 < 1$) to unstable ($R_1 > 1$), while creating the mosquito-free equilibrium (MFE) which is stable when ($R_0^{(TV)} < 1$) which in turn changes its stability at $R_0^{(TV)} = 1$ and becomes unstable ($R_0^{(TV)} > 1$) and create a stable coexistent equilibrim (CE). A similar double trans-critical bifurcation is observed in the perfect maternal transmission situation ($\beta_v = 1$).*

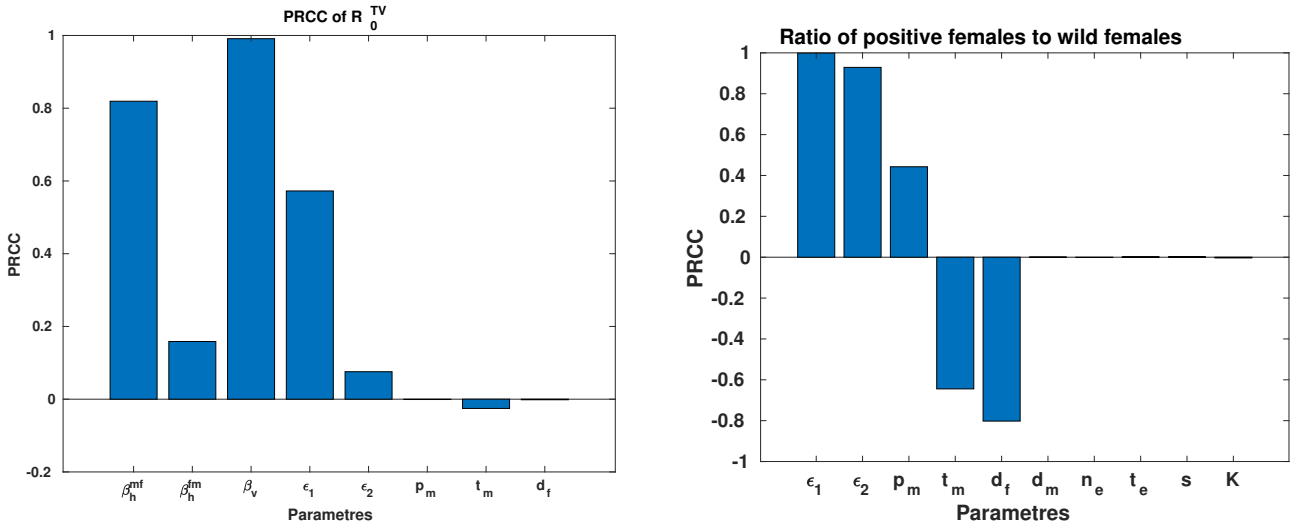

(a) **(b)**

Figure 2. (a) Effects of varying the parameters on the target reproduction number $\mathcal{R}_0^{(TV)}$. The ranges for the parameters are : β_h^{mf}, $\beta_h^{fm} \in [0.01\ 0.5]$; $\beta_v \in [0.01\ 0.99]$; ϵ_1, $\epsilon_2 \in [0.5\ 1.5]$; $p_m \in [0.6\ 1]$; $t_m \in [2\ 5]$; $d_f \in [1/43.2\ 1/23.4]$. (b) Effects of the parameters of the model of the ratio of *MB*-positive females to wild females. The ranges for the parameters are: $\beta_h^{mf} = \beta_h^{fm} = 0.35; \beta_v = 0.75$; ϵ_1, $\epsilon_2 \in [0.5\ 1.5]$; $p_m \in [0.6\ 1]$; $t_m \in [2\ 5]$; d_f, $d_m \in [0.01\ 0.05]$; $t_e \in [7.7\ 31]$; $n_e \in [0.8\ 6]$; $s \in [0.157\ 0.729]$; $K \in [200000\ 500000]$.

We are recalling that the stability of the coexistence equilibrium when $R_1 > 1$ & $\mathcal{R}_0^{(TV)} > 1$ indicates that the situation will converge to the coexistence of *MB*-infected and wild mosquitoes whenever that condition is verified.

As the population of mosquitoes always exists, we extrapolate the instability of the zero equilibrium and assume $R_1 > 1$. Moreover, the stability condition of the *MB*-complete infection steady state, $\beta_v = 1$, shows that a 100% prevalence of *MB*-infected mosquitoes can be achieved only with perfect vertical transmission ($\beta_v = 1$). Furthermore, we can deduce factors influencing the extinction of *MB*-infected mosquitoes by evaluating $\mathcal{R}_0^{(TV)}$.

To assess the effect of the model parameters on the target reproduction number $\mathcal{R}_0^{(TV)}$, we carry out a PRCC sensitivity analysis of $\mathcal{R}_0^{(TV)}$ whose graphical representation is depicted in Figure 2a. As expected, the sensitivity analysis in Figure 2 shows that the parameters having the greater influence on the spread of the *MB*-infected mosquitoes are the efficiency of vertical transmission (β_v), the male-to-female horizontal transmission efficiency (β_h^{mf}) and the attractiveness of *MB*-positive males. On the

other hand, it is interesting to note the low influence of the female-to-male horizontal transmission efficiency (β_h^{fm}). The low influence of the female-to-male transmission efficiency can, however, be explained as follows. In fact, the infection of a male will impact the spread of *Microsporidia MB* only if the male mate a second time with and infects a susceptible female before dying. Thus, the impact of the female-to-male transmission depends on the male-to-female transmission efficiency, which acts a double way and has a strong influence on the spread of *Microsporidia MB*. It is worth retaining from this analysis that the female-to-male horizontal transmission acts on the spread of *Microsporidia MB* only when we consider multiple mating activities for males.

To assess which parameter ranges correspond to the extinction or persistence of the *MB*-infected mosquitoes, we evaluate the values of our target reproduction number $\mathcal{R}_0^{(TV)}$, using data ranges obtained from field experiments and presented in Table 1. The assessment of the variation focused on the most influencing parameters, male-to-female and female-to-male horizontal transmission efficiencies β_h^{mf}, β_h^{fm}, the vertical transmission efficiency β_v and is presented in Figure 3. To plot the graph in Figure 3, we generate random numbers for each of the parameters β_h^{mf}, β_h^{fm}, and β_v from the continuous uniform distributions on the intervals β_h^{mf}, $\beta_h^{mf} \in [0.01\ 1]$; $\beta_v \in [0.01\ 0.99]$. Then, the target reproduction number $R_0^{(TV)}$ is computed for each triplet $(\beta_h^{mf}, \beta_h^{fm}, \beta_v)$, is plotted in blue for values lower than 1 and plotted in red for values higher than 1.

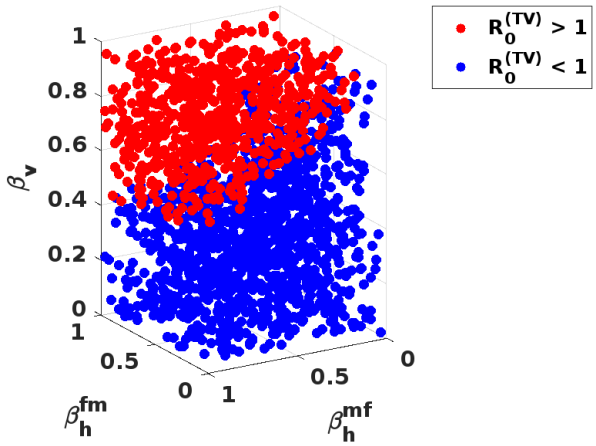

Figure 3. Variation of the target reproduction number $\mathcal{R}_0^{(TV)}$. The ranges for the parameters are : β_h^{mf}, $\beta_h^{fm} \in [0.01\ 1]$; $\beta_v \in [0.01\ 0.99]$; $\epsilon_1 = \epsilon_2 = 1$; $p_m = 0.7665$; $t_m = 3$ and $p_f = 0.5$.

Figure 3 shows the importance of having the horizontal transmission combined with the vertical transmission for the spread of *Microsporidia MB*. In fact, we observe special cases with high vertical transmission efficiency like $\beta_h^{mf} = 0.035$, $\beta_h^{fm} = 0.09$ and $\beta_v = 0.97$ leading to $\mathcal{R}_0^{(TV)} < 1$, thus extinction of *MB*-infected mosquitoes. Moreover, even with high male-to-female and female-to-male horizontal transmission efficiencies $\beta_h^{mf} = 0.98$, $\beta_h^{fm} = 0.99$, and a lower vertical transmission efficiency $\beta_v = 0.37$, we get $\mathcal{R}_0^{(TV)} < 1$, thus extinction of *MB*-infected mosquitoes. Overall, for male-to-female and female-to-male horizontal transmission efficiencies in the range β_h^{mf}, $\beta_h^{fm} \in [0, 0.5]$, a vertical transmission efficiency at least higher than 0.5 is necessary to ensure the persistence of *MB*-infected mosquitoes.

In the case of stable endemic equilibrium, meaning $\mathcal{R}_0^{(TV)} > 1$, we have computed the coexistence

equilibrium values which give the number of *MB*-positive and wild mosquitoes at the equilibrium. Therefore, we can deduce the prevalence of *MB*-infected mosquitoes expressed as :

$$p = \frac{\overline{F_p} + \overline{F_p}^m + \overline{M_p}}{\overline{F_p} + \overline{F_n} + \overline{F_p}^m + \overline{F_n}^m + \overline{M_p} + \overline{M_n}};$$

where $\overline{F_p}$, $\overline{F_p}^m$, $\overline{M_p}$, $\overline{F_n}$, $\overline{F_n}^m$ and $\overline{M_n}$ are defined in (4.2). We provide a numerical analysis of the variation of the prevalence of *MB*-infected mosquitoes in Figure 4. The method used to plot the graph in Figure 4 is the same as described above for Figure 3. Recalling that the mosquitoes collected from the field and screened for the presence of *Microsporidia* have shown a prevalence of *MB*-infected mosquitoes lower than 15% [4], we have highlighted in red (Figure 4), vertical and horizontal transmission efficiencies complying with a prevalence of *MB*-positive mosquitoes lower than 15%. We realise according to Figure 4 that a low prevalence of *MB*-infected mosquitoes is associated with a low male-to-female horizontal transmission efficiency.

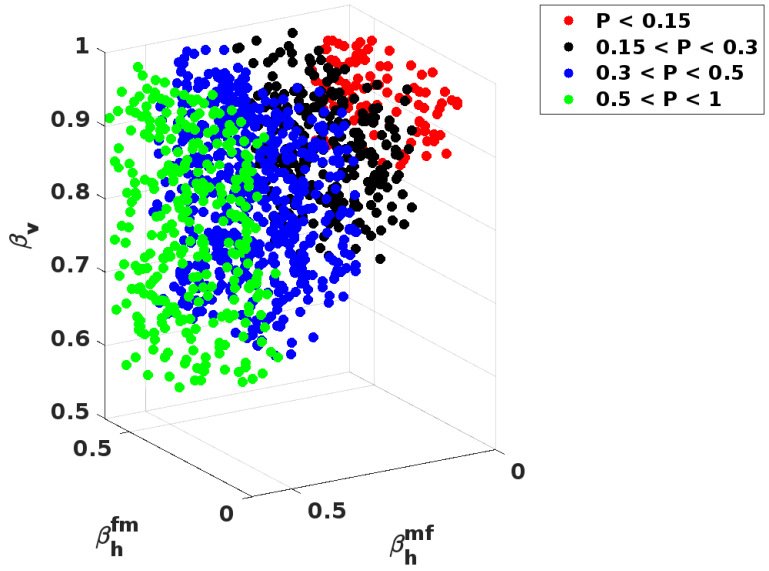

Figure 4. Variation of the prevalence of *MB*-infected mosquitoes. Parameters are chosen following a continuous uniform distribution in the following ranges: β_h^{mf}, $\beta_h^{fm} \in [0.01\ 0.6]$; $\beta_v \in [0.01\ 0.99]$; $\epsilon_1 = \epsilon_2 = 1$; $p_m = 0.7665$; $t_m = 3$; $d_f = 0.0345$; $d_m = 0.047$; $n_e = 1$ and $t_e = 19.35$, $s = 0.443$; $K = 200,000$ and $p_f = 0.5$.

Briefly, the analysis is showing that the main parameters driving the spread of the symbiont are the efficiencies of vertical and horizontal transmission. In addition, the model gives parameter ranges (Figure 4) in agreement with the low prevalence reported from field experiments [3, 4]. Assuming that the efficiencies of horizontal and vertical transmission are constant in nature, we are exploring secondary factors contributing to the spread of *MB*-infected mosquitoes. Let us fix $\beta_v = 0.7$, $\beta_h^{mf} =$

0.35, $\beta_h^{fm} = 0.35$ and consider the ratio of *MB*-infected females to wild females

$$ratio = \frac{F_p + F_p^m}{F_n + F_n^m};$$

in the condition of stability of the coexistence equilibrium $\left(R_1 > 1 \text{ and } \mathcal{R}_0^{(TV)} > 1\right)$. We carry out a PRCC sensitivity analysis of the *ratio* and the graphical output is represented in Figure 2b. Figure 2b shows that the most influencing factors are the attractiveness of *MB*-positive males compared to wild males for wild females ϵ_1, the attractiveness of wild males compared to *MB*-positive males for *MB*-positive females ϵ_2, the average time before mating t_m and the female death rate d_f.

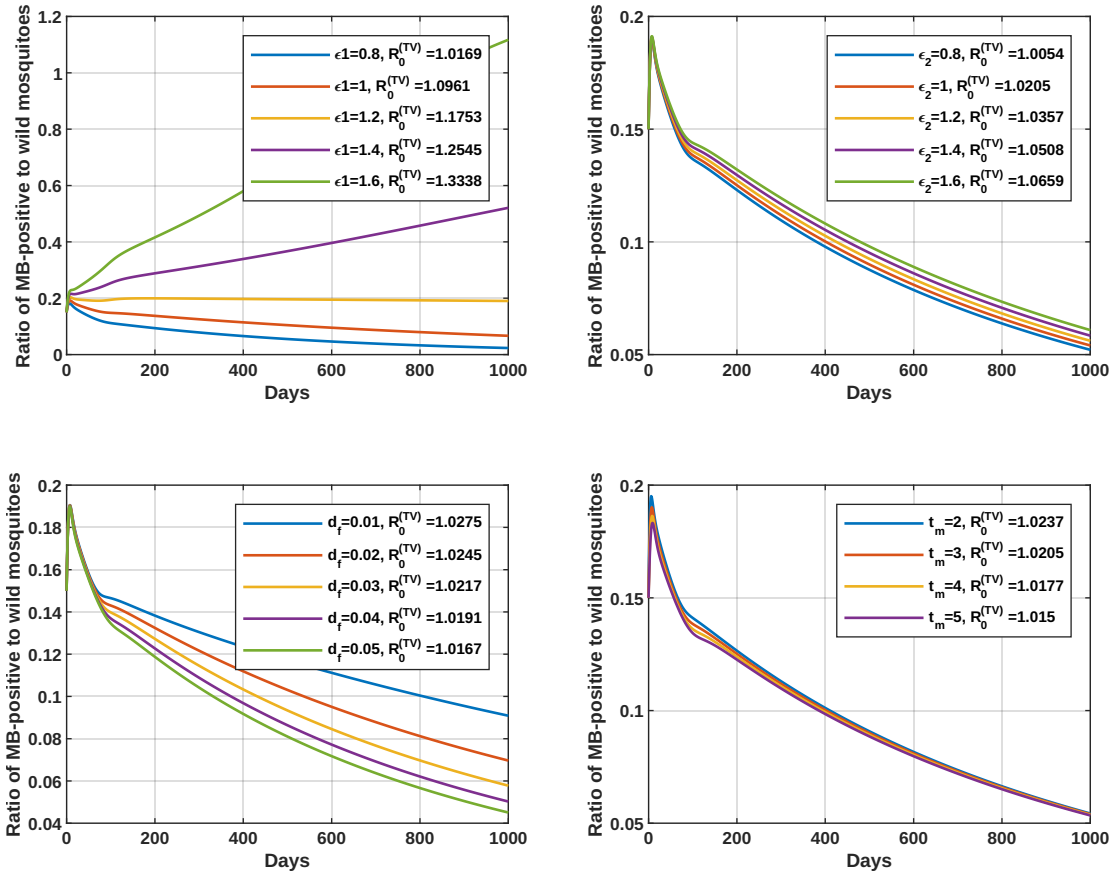

Figure 5. Effect of varying the attractiveness of *MB*-positive males to wild females ϵ_1, the attractiveness of wild males to *MB*-positive females ϵ_1, the female death rate d_f and the average time to mating t_m on the ratio of *MB*-positive females to wild females. The values of the remaining parameters are: $\beta_h^{mf} = \beta_h^{fm} = 0.35$; $\beta_v = 0.7$; $p_m = 0.7665$; $d_m \in [0.01\ 0.05]$, $t_e = 19.35$, $n_e = 1$, $s = 0.72$, $K = 200,000$. Also, $\epsilon_1 = 1$; $\epsilon_2 = 1$; $d_f = 0.0345$, $t_m = 3$, respectively for graphs where those parameters are considered constants.

In addition, the *ratio* increases with reduced female mortality and a reduced average time for mating and increases with higher attractiveness ϵ_1 and ϵ_2. For a clear visualization of the effects of ϵ_1, ϵ_2, d_f and d_m on the variation of the *ratio*, Figure 5 depicts the time variation of the ratio for different sets of

parameters.

5. Proof of analytical results

5.1. Computation of the target reproduction number

We are computing the target reproduction number using the method described in [31]. The compartments made up of infected mosquitoes are: $(F_p,\ F_p^m,\ \mathcal{E}_p,\ M_p)$. We label those compartments by 1, 2, 3, and 4, respectively. Let J be the Jacobian matrix of system (2.1), linearized at the disease-free state. The target reproduction number is obtained using the decomposition $J = J_{\tilde{\mathcal{F}}} - J_{\tilde{\mathcal{V}}}$ where $J_{\tilde{\mathcal{F}}}$ and $J_{\tilde{\mathcal{V}}}$ are the Jacobian matrices of $\tilde{\mathcal{F}}$ and $\tilde{\mathcal{V}}$, respectively, evaluated at the *MB*-free equilibrium. If we set $z = n_e\beta_v F_p^m\,(1 - \mathcal{E}/K)$, then $\tilde{\mathcal{F}}$ and $\tilde{\mathcal{V}}$ are defined by:

$$\tilde{\mathcal{F}} = \begin{pmatrix} z \\ 0 \\ 0 \\ 0 \end{pmatrix} \text{ and } \tilde{\mathcal{V}} = \begin{bmatrix} \dfrac{s}{t_e}\mathcal{E}_p \\ -\dfrac{sp_f}{t_e}\mathcal{E}_p + \left(\dfrac{d_f t_m + p_m}{t_m}\right)F_p \\ -\dfrac{p_m}{t_m}F_p - \dfrac{p_m}{t_m}\beta_h^{mf}\dfrac{\epsilon_1 M_p}{M_p + M_n}F_n + d_f F_p^m \\ -\dfrac{s}{t_e}(1-p_f)\mathcal{E}_p - \dfrac{p_m}{t_m}F_p\beta_h^{fm}\dfrac{\epsilon_2 M_n}{M_p + M_n} + d_m M_p \end{bmatrix}.$$

Let $J_{\tilde{\mathcal{F}}}$ and $J_{\tilde{\mathcal{V}}}$ be the Jacobian matrices of $\tilde{\mathcal{F}}$ and $\tilde{\mathcal{V}}$ evaluated at the *MB*-free equilibrium, respectively. Then, straightforward computations lead to

$$J_{\tilde{\mathcal{F}}}J_{\tilde{\mathcal{V}}}^{-1} = \frac{n_e\beta_v}{R_1}\begin{bmatrix} \dfrac{\Delta_1}{d} & \dfrac{\Delta_2}{d} & \dfrac{1}{d_f} & \dfrac{u}{d_f d_m} \\ 0 & 0 & 0 & 0 \\ 0 & 0 & 0 & 0 \\ 0 & 0 & 0 & 0 \end{bmatrix}; \tag{5.1}$$

where,

$$\alpha = d_f + \frac{p_m}{t_m}; \qquad u = \frac{p_m\beta_h^{mf}\epsilon_1 F_n^*}{t_m M_n^*}; \qquad \Delta_1 = \frac{sp_f(p_m d_m + uvt_m}{t_e t_m} + \frac{\alpha us(1-p_f)}{t_e};$$

$$d = \frac{sd_f d_m\alpha}{t_e}; \qquad v = \frac{p_m\epsilon_2\beta_h^{fm}}{t_m}; \qquad \Delta_2 = \frac{s}{t_e}\left(\frac{p_m d_m + uvt_m}{t_m}\right).$$

Following [31], the target reproduction number corresponding to the target matrix $J_{\tilde{\mathcal{F}}}J_{\tilde{\mathcal{V}}}^{-1}$ is given

by $\mathcal{R}_0^{(TV)} = \rho(J_{\tilde{\mathcal{F}}} J_{\mathcal{V}}^{-1})$. That is,

$$\mathcal{R}_0^{(TV)} = \frac{n_e \beta_v \Delta_1}{R_1 d} = \beta_v \left(1 + \epsilon_1 \beta_h^{mf} + \frac{p_m p_f \epsilon_1 \beta_h^{mf} \epsilon_2 \beta_h^{fm}}{(1 - p_f)\left(t_m d_f + p_m\right)} \right). \tag{5.2}$$

5.2. *Proof of Theorem 1*

The associated Cauchy problem to the model (2.1) has a unique solution since the right-hand side is differentiable for all time and hence locally Lipschitz on its definition domain. To prove the positiveness of the solution of (2.1) when the initial conditions are positive, we demonstrate that this system is monotone. In fact, System (2.1) can also be written in the form

$$\frac{dP(t)}{dt} = \mathcal{M} P(t); \tag{5.3}$$

where,

$$\mathcal{M} = \begin{pmatrix} -(d_f + \frac{p_m}{t_m}) & 0 & 0 & 0 & \frac{s p_f}{t_e} & 0 & 0 & 0 \\ 0 & -(d_f + \frac{p_m}{t_m}) & 0 & 0 & 0 & \frac{s p_f}{t_e} & 0 & 0 \\ \frac{p_m}{t_m} & \frac{\alpha p_m}{t_m} & -d_f & 0 & 0 & 0 & 0 & 0 \\ 0 & \frac{(1-\alpha) p_m}{t_m} & 0 & -d_f & 0 & 0 & 0 & 0 \\ 0 & 0 & \gamma n_e \beta_v & 0 & -\frac{s}{t_e} & 0 & 0 & 0 \\ 0 & 0 & \gamma n_e (1 - \beta_v) & \gamma n_e & 0 & -\frac{s}{t_e} & 0 & 0 \\ 0 & 0 & 0 & 0 & \frac{s(1-p_f)}{t_e} & 0 & -d_m & \beta \\ 0 & 0 & 0 & 0 & 0 & \frac{s(1-p_f)}{t_e} & 0 & -d_m - \beta \end{pmatrix}$$

with $\alpha = \beta_h^{mf} \dfrac{\epsilon M_p}{M_p + M_n}$; $\beta = \dfrac{p_m}{t_m} \beta_h^{fm} \dfrac{F_p}{F_p + F_n}$ and $\gamma = 1 - \dfrac{\mathcal{E}}{K}$;

and,

$$P(t) = (F_p(t), F_n(t), F_p^m(t), F_n^m(t), \mathcal{E}_p(t), \mathcal{E}_n(t), M_p(t), M_n(t))^\intercal.$$

All the non-diagonal terms of the matrix $\mathcal{M}$ are non-negative. Thus, M is a Metzler matrix and the system (5.3) is monotone. Hence, $\mathbb{R}_+^8$ is invariant by the flow of the system (5.3). We conclude the positiveness of the solution of the system for initial positive conditions. Let us denote by

$$F = F_p + F_n,\ F^m = F_p^m + F_n^m,\ \mathcal{E} = \mathcal{E}_p + \mathcal{E}_n \text{ and } M = M_p + M_n; \tag{5.4}$$

and demonstrate the boundedness of the solution of (2.1). According to (2.1), F, F^m, $\mathcal{E}$ and M satisfy the following equations:

$$\begin{cases} \dfrac{dF}{dt} = \dfrac{s}{t_e}p_f\mathcal{E} - (d_f + \dfrac{p_m}{t_m})F; & \dfrac{dF^m}{dt} = \dfrac{p_m}{t_m}F - d_fF^m; \\ \dfrac{d\mathcal{E}}{dt} = n_eF^m(1 - \dfrac{\mathcal{E}}{K}) - \dfrac{s}{t_e}\mathcal{E}; & \dfrac{dM}{dt} = \dfrac{s}{t_e}(1 - p_f)\mathcal{E} - d_mM. \end{cases} \tag{5.5}$$

First of all,

$$\mathcal{E}(t) \leq K \text{ for all time } t \text{ in the domain.} \tag{5.6}$$

Next, using (5.6), F can be constrained as follows.

$$\frac{dF}{dt} \leq \frac{s}{t_e}p_fK - d_fF - \frac{p_m}{t_m}F; \tag{5.7}$$

Hence,

$$\limsup_{t\to+\infty} F(t) \leq \frac{t_m s p_f K}{t_e(d_f t_m + p_m)}.$$

This prove the boundedness of the unmated female mosquito population $F(t) \leq (t_m s p_f K)/(t_e(d_f t_m + p_m))$. Using the same reasoning and equations (5.5), we show that

$$F^m(t) \leq \frac{p_m s p_f K}{d_f t_e\left(t_m d_f + p_m\right)} \text{ and } \frac{dM}{dt} \leq \frac{s(1 - p_f)K}{t_e} - d_mM.$$

Therefore, the population of model (2.1) starts and remain in the bounded set Δ.

5.3. Computation of the equilibria

The System (2.1) admits the trivial equilibrium $ZE = (0,\ 0,\ 0,\ 0,\ 0,\ 0,\ 0,\ 0)$ corresponding to the extinction of the mosquito population. The proof for the existence of the MB-free equilibrium (MFE) and the coexistence equilibrium (CE) are given below.

We denote by MFE the MB-free equilibrium corresponding to the steady state of System (2.1), where all the MB-infected components are zero while the uninfected components are positive. Therefore, those uninfected components satisfy the following equations.

$$\begin{cases} 0 = \dfrac{s}{t_e}p_f\mathcal{E}_n - \left(\dfrac{d_f t_m + p_m}{t_m}\right)F_n; & 0 = \dfrac{p_m}{t_m}F_n - d_fF_n^m; \\ 0 = n_eF_n^m\left(1 - \dfrac{\mathcal{E}_n}{K}\right) - \dfrac{s}{t_e}\mathcal{E}_n; & 0 = \dfrac{s}{t_e}(1 - p_f)\mathcal{E}_n - d_mM_n. \end{cases} \tag{5.8}$$

By solving (5.8), the *MB*-free equilibrium is defined such that:

$$\begin{cases} F_n = \dfrac{t_m s p_f}{t_e(d_f t_m + p_m)}\mathcal{E}_n; & F_n^m = \dfrac{p_m}{t_m d_f}F_n; \\ \\ M_n = \dfrac{s}{t_e d_m}(1-p_f)\mathcal{E}_n; & 0 = \dfrac{s}{t_e}\mathcal{E}_n\left(\dfrac{n_e p_m p_f}{d_f\left(t_m d_f + p_m\right)}\left(1-\dfrac{\mathcal{E}_n}{K}\right)-1\right). \end{cases} \tag{5.9}$$

Using the last expression of (5.9) and considering $\mathcal{E}_n \neq 0$, we have :

$$1-\frac{\mathcal{E}_n}{K} = \frac{d_f\left(t_m d_f + p_m\right)}{n_e p_m p_f}.$$

Then, the *MB*-free equilibrium verify :

$$\mathcal{E}_n = K\left(1-\frac{d_f\left(t_m d_f + p_m\right)}{n_e p_m p_f}\right) = K\left(1-\frac{1}{R_1}\right).$$

We denote by *CE* the coexistence equilibrium corresponding to the steady state of System (2.1), where the wild mosquitoes and the MB-positive mosquitoes coexist. The equilibrium points of the system (2.1). We can easily observe that $\mathcal{E} = \mathcal{E}_p + \mathcal{E}_n$, $F^m = F_p^m + F_n^m$ and $M = M_p + M_n$ verify respectively:

$$1-\frac{\mathcal{E}}{K} = \frac{d_f\left(t_m d_f + p_m\right)}{n_e p_m p_f} = \frac{1}{R_1};\ F^m = \frac{p_m s p_f}{d_f t_e\left(t_m d_f + p_m\right)}\mathcal{E} \text{ and } M = \frac{s(1-p_f)}{t_e d_m}\mathcal{E}. \tag{5.10}$$

Next, using (5.10), and the equation $d\mathcal{E}_p/dt = 0$ one has

$$F_p^m = \frac{s p_m p_f}{t_e \beta_v d_f\left(t_m d_f + p_m\right)}\mathcal{E}_p. \tag{5.11}$$

Using the expression of $F^m = F_p^m + F_n^m$ given in (5.10), we deduce the expression of F_n^m :

$$F_n^m = \frac{p_m s p_f}{d_f t_e\left(t_m d_f + p_m\right)}\left(\mathcal{E}_n + \left(1-\frac{1}{\beta_v}\right)\mathcal{E}_p\right). \tag{5.12}$$

From the equations $dF_p^m/dt = 0$ and $dF_n^m/dt = 0$, we have

$$\frac{M_p}{M_p + M_n} = \frac{1-\beta_v}{\epsilon_1 \beta_v \beta_h^{mf}}\frac{\mathcal{E}_p}{\mathcal{E}_n}.$$

In addition, from the equation $dM_p/dt = 0$, we deduce that

$$M_p = \frac{s(1-p_f)\left(1+\dfrac{p_m p_f \epsilon_2 \beta_h^{fm}}{(1-p_f)\left(t_m d_f + p_m\right)}\right)\mathcal{E}_p}{t_e d_m \left(1+\dfrac{p_m p_f \epsilon_2 \beta_h^{fm}}{(1-p_f)\left(t_m d_f + p_m\right)}\dfrac{R_1 \mathcal{E}_p}{K(R_1-1)}\right)}. \tag{5.13}$$

Equating (5.12) and (5.13) gives

$$\frac{(1-\beta_v)s(1-p_f)\mathcal{E}}{t_e d_m \epsilon_1 \beta_v \beta_h^{mf}}\frac{\mathcal{E}_p}{\mathcal{E}_n} = \frac{s(1-p_f)\left(1+\dfrac{p_m p_f \epsilon_2 \beta_h^{fm}}{(1-p_f)\left(t_m d_f + p_m\right)}\right)\mathcal{E}_p}{t_e d_m \left(1+\dfrac{p_m p_f \epsilon_2 \beta_h^{fm}}{(1-p_f)\left(t_m d_f + p_m\right)}\dfrac{R_1 \mathcal{E}_p}{K(R_1-1)}\right)}. \tag{5.14}$$

Then, after some computations, Equation (5.14) is equivalent to :

$$\mathcal{E}_p = K\left(1-\frac{1}{R_1}\right)\left(\frac{-1+R_0^{(TV)}}{B(1-\beta_v)+\epsilon_1\beta_v\beta_h^{mf}(1+B)}\right). \tag{5.15}$$

where $B = \dfrac{p_m p_f \epsilon_2 \beta_h^{fm}}{(1-p_f)\left(t_m d_f + p_m\right)}$.
Finally, we can easily obtain the coexistence equilibrium given in (4.2) by replacing $\mathcal{E}_p$ giving by (5.15) in (5.10)–(5.13).

5.4. Proof of Theorem 2 (local asymptotic stability of the equilibria.)

To simplify the presentation in the following subsections, we study the stability of a generic matrix $M(a,\ b,\ c,\ d,\ e,\ f)$ defined by :

$$M(a,\ b,\ c,\ d,\ e,\ f) = \begin{pmatrix} a & 0 & b & 0 \\ \dfrac{sp_f}{t_e} & -\left(\dfrac{d_f t_m + p_m}{t_m}\right) & 0 & 0 \\ 0 & \dfrac{p_m}{t_m} f & -d_f & c \\ \dfrac{s(1-p_f)}{t_e} & d & 0 & e \end{pmatrix} = \left[\begin{array}{c|c} M_1 & M_2 \\ \hline M_3 & M_4 \end{array}\right]; \tag{5.16}$$

where $a,\ b,\ c,\ d,\ e,$ and f are real numbers, $a \neq 0$ and the matrices $M_i, i = 1,2,3,4$ are 2×2. Clearly, M is a Metzler matrix because M is a square matrix with non-negative off-diagonal entries.

According to [33], M is Metzler stable if and only if M_1 and $M_4 - M_3M_1^{-1}M_2$ are Metzler stable matrices. Obviously, M_1 has all its eigenvalues negative and is Metzler stable whenever $a < 0$. In addition,

$$M_4 - M_3M_1^{-1}M_2 = \begin{pmatrix} d_f\left(-1 - \dfrac{fbsR_1}{at_en_e}\right) & c \\ -\dfrac{bs}{at_e}\left(1 - p_f + \dfrac{dp_ft_m}{d_ft_m + p_m}\right) & e \end{pmatrix}.$$

To determine the signs of the real part of the eigenvalues of the 2×2 matrix, $M_4 - M_3M_1^{-1}M_2$, we simply analyse the sign of its trace and determinant. Two eigenvalues of $M_4 - M_3M_1^{-1}M_2$ have negative real parts if and only if the trace is negative and the determinant is positive. The trace and determinant of $M_4 - M_3M_1^{-1}M_2$ are :

$$\begin{cases} trace(M_4 - M_3M_1^{-1}M_2) & = d_f\left(-1 - \dfrac{fbsR_1}{at_en_e}\right) + e; \\ \\ det(M_4 - M_3M_1^{-1}M_2) & = ed_f\left(-1 - \dfrac{bsR_1}{at_en_e}\right) + \dfrac{cbs}{at_e}\left(1 - p_f + \dfrac{dp_ft_m}{d_ft_m + p_m}\right). \end{cases} \tag{5.17}$$

In summary, M is a Metzler stable matrix whenever $a < 0$, $trace(M_4 - M_3M_1^{-1}M_2) < 0$ and $det(M_4 - M_3M_1^{-1}M_2) > 0$. Thus, under the above-mentioned conditions, the real part of any eigenvalue of M is strictly negative. This will serve in the following subsections to derive the stability of the equilibria.

5.4.1. Local asymptotic stability of the equilibria ZE, MFE and CIE

We prove the stability of the ZE equilibrium by determining the signs of the eigenvalues of the linearized matrix of the system (2.1) at the point ZE. The Jacobian matrix of the system (2.1) at point MFE is the following block matrix;

$$M_{ze} = \begin{pmatrix} U & 0 \\ W & V \end{pmatrix};$$

where,

$$U = M\left(-\frac{s}{t_e},\ n_e\beta_v,\ 0,\ 0,\ -d_m,\ 1\right);\ V = M\left(-\frac{s}{t_e},\ n_e,\ 0,\ 0,\ -d_m,\ 1\right) \text{ and } W = \begin{pmatrix} 0 & 0 & n_e(1-\beta_v) & 0 \\ 0 & 0 & 0 & 0 \\ 0 & 0 & 0 & 0 \\ 0 & 0 & 0 & 0 \end{pmatrix}. \tag{5.18}$$

Then, the eigenvalues of M_{ze} are the union of the eigenvalues of U and V, and the ZE equilibrium is asymptotically stable when U and V are Metzler stable. Using the computations done for the generalized matrix (5.16), U is Metzler stable if and only if

$$-d_m - d_f(1 - \beta_vR_1) < 0 \text{ and } d_md_f(1 - \beta_vR_1) > 0.$$

Similarly, V is Metzler stable if and only if

$$-d_m - d_f(1 - R_1) < 0 \text{ and } d_m d_f(1 - R_1) > 0.$$

Clearly, if $R_1 < 1/\beta_v$, then U Metzler stable. Similarly, if $R_1 < 1$, V is Metzler stable. Finally, since $\beta_v \leq 1$, we conclude the local asymptotic stability of the ZE equilibrium when $R_1 < 1$ and the instability when $R_1 > 1$.

The proof of the stability of MFE is performed similarly, by noticing that The Jacobian matrix of the system (2.1) at MFE is the following block matrix:

$$M_{mfe} = \begin{pmatrix} A & 0 \\ * & D \end{pmatrix};$$

where (*) denotes a 4×4 matrix, which is not needed for this proof, and

$$A = M\left(-\frac{s}{t_e},\ \frac{n_e\beta_v}{R_1},\ \epsilon_1\beta_h^{mf}\frac{p_m}{t_m}\frac{F_n^*}{M_n^*},\ \epsilon_2\beta_h^{fm}\frac{p_m}{t_m},\ -d_m,\ 1\right);\ D = M\left(-\frac{s}{t_e}R_1,\ \frac{n_e}{R_1},\ 0,\ 0,\ -d_m,\ 1\right). \quad (5.19)$$

By proceeding in the same way as above, for the matrices U and V, it can be easily shown that the matrice A is Metzler stable whenever $\mathcal{R}_0^{(TV)} < 1$ and the matrice D is Metzler stable whenever $R_1 > 1$ and the proof is achieved.

We proceed similarly as above for the proof of the local stability of the CIE. The Jacobian matrix of System (2.1) at CIE is a block matrix

$$M_{cie} = \begin{pmatrix} X & Y \\ 0 & Z \end{pmatrix}$$

where Y is a 4×4 matrix, which is not needed in this proof,

$$X = M\left(-\frac{s}{t_e}R_1,\ \frac{n_e}{R_1},\ 0,\ 0,\ -d_m,\ 1\right); \quad (5.20)$$

and

$$Z = M\left(-\frac{s}{t_e},\ \frac{n_e}{R_1},\ 0,\ 0,\ -d_m - \frac{p_m}{t_m}\epsilon_2\beta_h^{fm}\frac{F_p^{**}}{M_p^{**}},\ 1 - \epsilon_1\beta_h^{mf}\right). \quad (5.21)$$

An analogous approach as above shows that X is Metzler stable whenever $R_1 > 1$ and Z is always Metzler stable.

5.4.2. Local asymptotic stability of CE

The Jacobian matrix M_{ce} of the system (2.1) at point CE is the matrix;

$$M_{ce} = \begin{pmatrix} -a_1 & 0 & a_2 & 0 & -a_3 & 0 & 0 & 0 \\ \frac{sp_f}{t_e} & -\frac{d_f t_m + p_m}{t_m} & 0 & 0 & 0 & 0 & 0 & 0 \\ 0 & \frac{p_m}{t_m} & -d_f & a_4 & 0 & a_5 & 0 & -a_6 \\ \frac{s(1-p_f)}{t_e} & a_7 & 0 & -a_8 & 0 & 0 & 0 & a_9 \\ -a_{10} & 0 & a_{11} & 0 & -a_{12} & 0 & \frac{n_e}{R_1} & 0 \\ 0 & 0 & 0 & 0 & \frac{sp_f}{t_e} & -\frac{d_f t_m + p_m}{t_m} & 0 & 0 \\ 0 & 0 & 0 & -a_6 & 0 & a_{13} & -d_f & a_6 \\ 0 & -a_7 & 0 & a_{14} & \frac{s(1-p_f)}{t_e} & 0 & 0 & -a_{15} \end{pmatrix}$$

where

$$a_1 = \frac{s}{t_e} + \frac{n_e \beta_v}{K} \overline{F_p^m}; \qquad a_2 = \frac{n_e \beta_v}{R_1};$$

$$a_3 = \frac{n_e \beta_v}{K} \overline{F_p^m}; \qquad a_4 = \epsilon_1 \beta_h^{mf} \frac{p_m}{t_m} \frac{\overline{M_n F_n}}{(\overline{M_p} + \overline{M_n})^2};$$

$$a_5 = \frac{p_m}{t_m} \epsilon_1 \beta_h^{mf} \frac{\overline{M_p}}{\overline{M_p} + \overline{M_n}}; \qquad a_6 = \epsilon_1 \beta_h^{mf} \frac{p_m}{t_m} \frac{\overline{M_p F_n}}{(\overline{M_p} + \overline{M_n})^2};$$

$$a_7 = \epsilon_2 \beta_h^{fm} \frac{p_m}{t_m} \frac{\overline{M_n}}{\overline{M_p} + \overline{M_n}} \qquad a_8 = d_m + a_{14};$$

$$a_9 = \epsilon_2 \beta_h^{fm} \frac{p_m}{t_m} \frac{\overline{F_p M_p}}{(\overline{M_p} + \overline{M_n})^2}; \qquad a_{10} = \frac{n_e \overline{F_n^m}}{K} + \frac{n_e (1-\beta_v)}{K} \overline{F_p^m};$$

$$a_{11} = \frac{n_e (1-\beta_v)}{R_1}; \qquad a_{12} = a_{10} + \frac{s}{t_e};$$

$$a_{13} = \frac{p_m}{t_m} \left(1 - \epsilon_1 \beta_h^{mf} \frac{\overline{M_p}}{\overline{M_p} + \overline{M_n}} \right); \qquad a_{14} = \epsilon_2 \beta_h^{fm} \frac{p_m}{t_m} \frac{\overline{F_p M_n}}{(\overline{M_p} + \overline{M_n})^2};$$

$$a_{15} = d_m + a_9.$$

We are using the method described in [34, 35] and proving that the linearized equation $w' = M_{ce} w$, $(w \in \Delta)$ has no solution of the form $w(t) = W \exp(z(t))$ with $W \in \mathbb{C}^8$, $z \in \mathbb{C}$, $Re z \geq 0$. This is equivalent to showing that

$$zW = M_{ce} W, \ W \in \mathbb{C}^8 \backslash \{0\}, \ z \in \mathbb{C} \Rightarrow Re z < 0.$$

Assuming $W\exp(z(t))$, $W = (W_1, W_2, W_3, W_4, W_4, W_6, W_7, W_8)$, $z \in \mathbb{C}$ $(Rez \geq 0)$; solution of the linearized system $w' = M_{ce}w$, we have :

$$\begin{cases} zW_1 &= -a_1W_1 + a_2W_3 - a_3W_5; \\ zW_2 &= \dfrac{sp_f}{t_e}W_1 - \left(\dfrac{d_f t_m + p_m}{t_m}\right)W_2; \\ zW_3 &= \dfrac{p_m}{t_m}W_2 - d_fW_3 + a_4W_4 + a_5W_6 - a_6W_8; \\ zW_4 &= \dfrac{s(1-p_f)}{t_e}W_1 + a_7W_2 - a_8W_4 + a_9W_8; \\ zW_5 &= -a_{10}W_1 + a_{11}W_3 - a_{12}W_5 + \dfrac{n_e}{R_1}W_7; \\ zW_6 &= \dfrac{sp_f}{t_e}W_5 - \left(\dfrac{d_f t_m + p_m}{t_m}\right)W_6; \\ zW_7 &= -a_6W_4 + a_{13}W_6 - d_fW_7 + a_6W_8; \\ zW_8 &= -a_7W_2 + a_{14}W_4 + \dfrac{s(1-p_f)}{t_e}W_5 - a_{15}W_8. \end{cases} \tag{5.22}$$

After some rearrangements, System (5.22) is equivalent to

$$(1 + F_i(z))W_i + G_i(W) = (HW)_i; \tag{5.23}$$

where

$$\begin{cases} F_1(z) &= \dfrac{t_e}{s}(z + a_3);\ F_2(z) = \dfrac{t_m}{d_f t_m + p_m}z;\ F_3(z) = \dfrac{1}{d_f}z;\ F_4(z) = \dfrac{1}{d_m}(z + a_{14}); \\ F_5(z) &= \dfrac{t_e}{s}(z + a_{10});\ F_6(z) = F_2(z);\ F_7(z) = F_3(z);\ F_8(z) = \dfrac{1}{d_m}(z + a_9). \end{cases} \tag{5.24}$$

and

$$\begin{cases} G_1(W) &= \dfrac{t_e}{s}a_3W_5;\ G_2(W) = 0;\ G_3(W) = \dfrac{a_6}{d_f}W_8 - \dfrac{a_4}{d_f}W_4;\ G_4(W) = \dfrac{a_8}{d_m}W_6 - \dfrac{a_7}{d_m}W_2; \\ G_5(W) &= \dfrac{t_e}{s}a_{10}W_1;\ G_6(W) = 0;\ G_7(W) = \dfrac{a_6}{d_f}W_4 - \dfrac{a_6}{d_f}W_8;\ G_8(W) = -\dfrac{a_{14}}{d_m}W_4. \end{cases} \tag{5.25}$$

and

$$H = \begin{pmatrix} 0 & 0 & \frac{t_e n_e \beta_v}{sR_1} & 0 & 0 & 0 & 0 & 0 \\ \frac{t_m s p_f}{t_e\left(d_f t_m + p_m\right)} & 0 & 0 & 0 & 0 & 0 & 0 & 0 \\ 0 & \frac{p_m}{t_m d_f} & 0 & 0 & 0 & \frac{a_5}{d_f} & 0 & 0 \\ \frac{s(1-p_f)}{t_e d_m} & \frac{a_7}{d_m} & 0 & 0 & 0 & 0 & 0 & 0 \\ 0 & 0 & \frac{t_e n_e (1-\beta_v)}{sR_1} & 0 & 0 & 0 & \frac{t_e n_e}{sR_1} & 0 \\ 0 & 0 & 0 & 0 & \frac{t_m s p_f}{t_e\left(d_f t_m + p_m\right)} & 0 & 0 & 0 \\ 0 & 0 & 0 & 0 & 0 & \frac{a_{13}}{d_f} & 0 & 0 \\ 0 & -\frac{a_7}{d_m} & 0 & 0 & \frac{s(1-p_f)}{t_e} & 0 & 0 & 0 \end{pmatrix}$$

H is a non-negative matrix and the coexistence equilibrium CE, $\overline{X}$ satisfies $\overline{X} = H\overline{X}$.
Let us recall that the objective is to prove that $Rez < 0$. We proceed by contradiction and assume that $Rez \geq 0$.
Because $G_2(W) = 0$, the second equation of (5.23) is

$$(1 + F_2(z))W_2 = (HW)_2. \tag{5.26}$$

We consider the euclidean norm$|.|$ in $\mathbb{C}$. By taking the norm on left and right sides of (5.26), we have :

$$\left|1 + F_2(z)\right||W_2| = \left|(HW)_2\right|. \tag{5.27}$$

Note that $\left|1 + F_2(z)\right| = \left|1 + \frac{t_m}{d_f t_m + p_m} z\right| > 1$ because we assumed that $Rez \geq 0$. In addition, since the components of the coexistence equilibrium $\overline{X}$ are all positive, it follows that if W represents a solution of the system (5.23), then it is possible to find a minimal positive real number c_0 such that

$$|W| \leq c_0 \overline{X}. \tag{5.28}$$

with

$$|W| = \left(|W_1|, |W_2|, |W_3|, |W_4|, |W_5|, |W_6|, |W_7|, |W_8|\right).$$

The existence of c_0 is straightforward by reasoning on a component-wise basis. In fact, for the two positive real numbers $|W_i|$ and $\overline{X}_i$, there is a positive number c_i such that $|W_i| \leq c_i \overline{X}_i$ (it suffices to take c_i to be any positive number greater than or equal to$|W_i| / \overline{X}_i$). Finally, choosing c_0 to be the minimum of c_i proves the inequality$|W| \leq c_0 \overline{X}$.
Therefore, using the fact that H is a non-negative matrix, the inequality (5.28) and $H\overline{X} = \overline{X}$, we deduce

from (5.27) that :

$$\Big|1 + F_2(z)\Big||W_2| = \Big|(HW)_2\Big| \leq H|W_2| \leq c_0 H(\overline{X})_2 = c_0(\overline{X})_2 = c_0\overline{F_p}; \tag{5.29}$$

Moreover, the inequality in (5.29) implies that $|W_2| \leq \dfrac{c_0}{\Big|1 + F_2(z)\Big|}(\overline{X})_2$. This contradicts the fact that c_0 is the minimum positive number satisfying (5.28). Thus, $Rez < 0$. Therefore, we have proved that all the eigenvalues of the characteristic equation associated with the linearized system around the coexistence equilibrium have a negative real part. We conclude the local asymptomatic stability of CE whenever it exists ($R_1 > 1$ and $\mathcal{R}_0^{(TV)} > 1$).

5.5. Global stability of the equilibria

5.5.1. Global stability of the ZE equilibrium

We use Lyapunov-LaSalle techniques to prove the global asymptotic stability of the equilibria. Let us denote $(\mathcal{E}_p,\ F_p,\ F_p^m,\ M_p,\ \mathcal{E}_n,\ F_n,\ F_n^m,\ M_n)$ by X, and consider the Lyapunov function $V : \Delta \to \mathbb{R}$ defined as follows :

$$V(X) = \mathcal{E} + \frac{1}{p_f}F + \frac{t_m d_f + p_m}{p_m p_f}F^m;$$

where $\mathcal{E} = \mathcal{E}_p + \mathcal{E}_n,\ F = F_p + F_n,$ and $F^m = F_p^m + F_n^m$.
Then, the time derivative of V is :

$$\begin{aligned}
\frac{dV}{dt} &= n_e F^m\left(1 - \frac{\mathcal{E}}{K}\right) - \frac{s}{t_e}\mathcal{E} + \frac{1}{p_f}\left(\frac{sp_f}{t_e}\mathcal{E} - \frac{t_m d_f + p_m}{t_m}F\right) + \frac{t_m d_f + p_m}{p_m p_f}\left(\frac{p_m}{t_m}F - d_f F^m\right);\\
&\leq n_e F^m - \frac{s}{t_e}\mathcal{E} + \frac{1}{p_f}\left(\frac{sp_f}{t_e}\mathcal{E} - \frac{t_m d_f + p_m}{t_m}F\right) + \frac{t_m d_f + p_m}{p_m p_f}\left(\frac{p_m}{t_m}F - d_f F^m\right);\\
&= n_e F^m\left(1 - \frac{1}{R_1}\right).
\end{aligned} \tag{5.30}$$

It follows that $dV/dt \leq 0$ whenever $R_1 < 1$. In addition, the largest invariant set contained in $\{X \in \Delta;\ dV/dt = 0\}$ is the trivial equilibrium ZE. Therefore, by LaSalle's invariance principle [36, 37], ZE is globally asymptotically stable in Δ, whenever $R_1 < 1$.

5.5.2. Global stability of the non-zero equilibrium

For the proof, we denote $(\mathcal{E},\ F,\ F^m, M)$ by Y, and consider the Lyapunov function defined as follows :

$$V(Y) = \mathcal{E} - \mathcal{E}^* - \mathcal{E}^* \ln\frac{\mathcal{E}}{\mathcal{E}^*} + \frac{1}{p_f}\left(F - F^* - F^* \ln\frac{F}{F^*}\right) + \frac{t_m d_f + p_m}{p_m p_f}\left(F^m - F^{m*} - F^{m*}\ln\frac{F^m}{F^{m*}}\right).$$

Then, the time derivative of V is :

$$\begin{aligned}\frac{dV}{dt} &= n_e F^m\left(1-\frac{\mathcal{E}}{K}\right)-\frac{s}{t_e}\mathcal{E}\left(1-\frac{\mathcal{E}^*}{\mathcal{E}}\right)+\frac{1}{p_f}\left(\frac{sp_f}{t_e}\mathcal{E}-\frac{t_m d_f+p_m}{t_m}F\right)\left(1-\frac{F^*}{F}\right)+\frac{t_m d_f+p_m}{p_m p_f}\left(\frac{p_m}{t_m}F-d_f F^m\right)\left(1-\frac{F^{m*}}{F^m}\right);\\ &= n_e F^m\left(1-\frac{1}{R_1}-\frac{\mathcal{E}}{K}+\frac{\mathcal{E}^*}{K}\right)+\frac{s}{t_e}\mathcal{E}^*\left(1-\frac{\mathcal{E}}{\mathcal{E}^*}\frac{F^*}{F}\right)+\frac{d_f t_m+p_m}{t_m p_f}F^*\left(1-\frac{F}{F^*}\frac{F^{m*}}{F^m}\right)+\frac{d_f(t_m d_f+p_m)}{p_m p_f}F^{m*}-n_e F^m\frac{\mathcal{E}^*}{\mathcal{E}}.\end{aligned}$$

From the computation of the equilibria of System (4.4), we have the following expressions :

$$\frac{\mathcal{E}^*}{K}=1-\frac{1}{R_1},\ \frac{d_f t_m+p_m}{t_m p_f}=\frac{s}{t_e}\frac{\mathcal{E}^*}{F^*}\ \text{ and }\ \frac{d_f(t_m d_f+p_m)}{p_m p_f}F^{m*}=\frac{n_e}{R_1}F^{m*}=\frac{s}{t_e}\mathcal{E}^*. \tag{5.31}$$

By using the equations in (5.31), we can simplify dV/dt and we get :

$$\begin{aligned}\frac{dV}{dt} &= n_e F^m\left(\frac{\mathcal{E}^*}{K}-\frac{\mathcal{E}}{K}+\frac{\mathcal{E}^*}{K}\right)+\frac{s}{t_e}\mathcal{E}^*\left(1-\frac{\mathcal{E}}{\mathcal{E}^*}\frac{F^*}{F}\right)+\frac{s}{t_e}\mathcal{E}^*\left(1-\frac{F}{F^*}\frac{F^{m*}}{F^m}\right)+\frac{n_e}{R_1}F^{m*}-\frac{n_e}{R_1}F^m\frac{\mathcal{E}^*}{\mathcal{E}}-\frac{n_e(R_1-1)}{R_1}F^m\frac{\mathcal{E}^*}{\mathcal{E}}\\ &= n_e F^m\frac{\mathcal{E}^*}{K}\left(2-\frac{\mathcal{E}}{\mathcal{E}^*}-\frac{\mathcal{E}^*}{\mathcal{E}}\right)+\frac{s}{t_e}\mathcal{E}^*\left(3-\frac{\mathcal{E}}{\mathcal{E}^*}\frac{F^*}{F}-\frac{F}{F^*}\frac{F^{m*}}{F^m}-\frac{F^m}{F^{m*}}\frac{\mathcal{E}^*}{\mathcal{E}}\right).\end{aligned}$$

From the inequality of arithmetic and geometric means, we have :

$$2-\frac{\mathcal{E}}{\mathcal{E}^*}-\frac{\mathcal{E}^*}{\mathcal{E}}\le 0 \text{ and } 3-\frac{\mathcal{E}}{\mathcal{E}^*}\frac{F^*}{F}-\frac{F}{F^*}\frac{F^{m*}}{F^m}-\frac{F^m}{F^{m*}}\frac{\mathcal{E}^*}{\mathcal{E}}\le 0;$$

with equality if and only if $\mathcal{E}=\mathcal{E}^*$, $F=F^*$, and $F^m=F^{m*}$.
Therefore, $dV/dt\le 0$, and $dV/dt=0$ if and only if $\mathcal{E}=\mathcal{E}^*$, $F=F^*$, and $F^m=F^{m*}$. Thus, it follows from the Lyapunov invariance principle, that $\lim_{t\to\infty}\mathcal{E}=\mathcal{E}^*$, $\lim_{t\to\infty}F=F^*$, and $\lim_{t\to\infty}F^m=F^{m*}$. Then, using the fourth equation of System (4.5), we also get $\lim_{t\to\infty}M=M^*$. Finally, we conclude the global asymptotic stability of the non-zero equilibrium (4.4) whenever $R_1>1$.

6. Discussion

The introduction of *MB*-infected mosquitoes into the wild mosquito population is foreseen as a promising malaria control strategy. Therefore, prior to investigating the effects of the presence of *MB* on the incidence of malaria as well as the design of release strategies to increase the prevalence of *MB*-infected mosquitoes, it is critical to understand and mimic the mechanism underpinning the low prevalence reported from field experiments [3, 4]. In this study, we formulated a deterministic compartmental model to understand the dynamics of the spread of *MB*-infected mosquitoes. The main features included in the model are the vertical transmission, the difference in horizontal transmission efficiencies from male to female and from female to male, the consideration of a unique mating for females and the use of contact conservation to define the number of males that are mating. In addition, the model considers both the adult and the immature stages by dividing the mosquito population into females, males and eggs. The dynamic of the model built on the previous assumptions is assessed by computing the basic reproduction number, and the equilibria and analysing their local asymptotic stability.

In summary, the analysis of the formulated model gives four steady states: a zero steady-state representing the situation where there is no mosquito that is stable when $R_1<1$, an *MB*-free state

representing the extinction of *MB*-positive mosquitoes that is stable when $R_1 > 1$ and $\mathcal{R}_0^{(TV)} < 1$, a coexistence state of *MB* and wild mosquitoes that is stable when $\beta_v < 1$, $R_1 > 1$ and $\mathcal{R}_0^{(TV)} > 1$, an *MB*-complete infection state representing the extinction of wild mosquitoes that is stable when $\beta_v = 1$ and $R_1 > 1$. Hence, a mosquito population entirely infected with *Microsporidia MB* is achievable only with a perfect vertical transmission. From the PRCC sensitivity analysis of the target reproduction number $\mathcal{R}_0^{(TV)}$ presented in Figure 2a, we observe that the most influencing parameters are the efficiencies of vertical and male-to-female horizontal transmission. Vertical transmission has the highest influence, followed by male-to-female horizontal transmission, while female-to-male horizontal transmission has a reduced influence because it relies on multiple mating for males. The high influence of vertical transmission has also been highlighted by Lipsitch et al. [10] while studying the dynamics of vertically and horizontally transmitted parasites. In addition, the numerical analysis highlights in Figure 4, the vertical and horizontal transmission efficiencies complying with a prevalence of *MB*-infected mosquitoes lower than 15% (as reported by [3, 4]). Assuming a vertical transmission efficiency, of around 75% on average, as reported from the field experiments [3, 4], we found that a low prevalence of *MB*-infected mosquitoes is associated with a low male-to-female horizontal transmission efficiency.

Overall, we recall that the use of *Microsporidia MB* as a bio-based agent for malaria control implies increasing its prevalence through releases of *MB*-infected mosquitoes. Thus, one aim of this study is to identify factors (excluding the efficiencies of vertical and horizontal transmission since it is difficult to act on their values biologically) that make *MB*-infected mosquitoes more likely to spread than wild mosquitoes. We found that the attractiveness of *MB*-positive males to wild females, the attractiveness of wild males to *MB*-positive females, the female death rate and the average time before mating are the most influencing parameters. Moreover, the ratio of *MB*-positive females to wild females decreases with female mortality. This can be interpreted as the alternative control measures are slowing the spread of *MB*-infected mosquitoes. However, because the alternative control measures are impacting both the *MB*-infected and wild mosquitoes, the benefits in terms of malaria case reduction while applying alternative control measures could still outweigh the benefits on the spread of *MB*-infected mosquitoes in case of high female mortality. It is worth noting that this result is obtained while assuming the same demographics for *MB* and wild mosquitoes.

This study analyzed the spread of *MB*-infected mosquitoes by assuming that all the malaria vectors can be infected with *Microsporidia*. However, Nattoh et al. [3] and Herren et al. [4] found the *Microsporidia* MB only in the population of *Anopheles Arabiensis*, *Funestus* and *Gambiae*. Thus, the results given here are relevant in areas like Kenya where those species are the primary malaria vectors [38]. Otherwise, further studies are required to assess whether *Microsporidia* MB can stably infect other *Anopheles* species such as *Anopheles moucheti* and *Anopheles nili* that are responsible for malaria transmission in other in forested and humid savannah areas of West and Central Africa [39]. In addition, the findings presented here are based on the assumption of a homogeneous spatial distribution of the *MB* and wild mosquitoes in nature. It is also useful to mention that the mosquito survival and birth rates, depend on seasonal dynamics of environmental variables, such as temperature, humidity and precipitation [40]. Especially, the life table characteristics of *Anopheles Arabiensis* [29] describes how the fluctuation in the temperature affects some traits of the mosquito like the egg survival rate, the egg development time and the male and female life expectancies. Thus, defining those parameters as temperature-dependent functions makes the model more realistic. At this end, we use data from the life table characteristics of *Anopheles Arabiensis* established by [29] to fit polynomials. The fitted polyno-

mials are presented in Table 4 and the correlation between the polynomials and the data is observed in Figure 6a.

Table 4. Temperature-dependent functions representing the egg survival and development rate, the male and female life expectancies.

Parameters	**Fitted functions**
Mean egg development rate ($1/t_e(t)$)	$-0.000093229181101T^3 + 0.00603712413277T^2 - 0.11735895569901T + 0.72290875910923$
Survival through immature stages (s)	$-0.00029007027885T^3 + 0.01453747156087T^2 - 0.15000026889234T - 0.04926327810974$
Male life expectancy ($1/d_m$)	$0.005824205636827T^3 - 0.428282677369847T^2 + 9.191145692872797T - 32.57385986107060$
Female life expectancy ($1/d_f$)	$0.009256095521957T^3 - 0.644047915039107T^2 + 12.68284422603250T - 32.24054475085850$

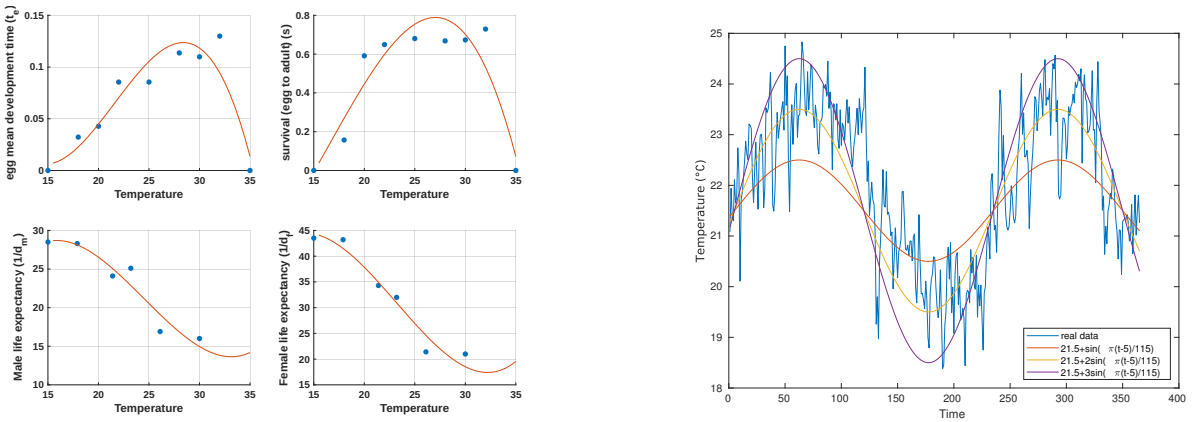

(a) **(b)**

Figure 6. (a) Temperature-dependent parameters obtained through a fitting procedure using a polynomial function to data obtained from the literature [29]. The corresponding functions are described in Table 4. (b) Time-dependent function representing yearly temperature fluctuations in Mwea, Kenya. The blue line is the value of the actual temperature collected. The graphs in orange, yellow and purple are the approximations at amplitude 1, 2 and 3 respectively.

It is important to mention that all the temperature-dependent polynomials obtained are positive for temperature values $T(t)$ in the range $[16,\ 35]$. Hence, for temperatures in this range, the temperature-dependent parameters are well-defined. The temperature is included, following the temperature in the Mwea region (Latitude=-0.778644 and Longitude =37.515316) and approximated with a time-dependent sine function

$$T(t) = 21.5 + a\sin(\frac{\pi}{115}(t-5));\ \ a \in \{1,2,3\}. \tag{6.1}$$

where t is the time, $T_0 = 21.5$ represents the average difference between highest and lowest temperatures, $2\times115 = 330$ *days* (11 months in a year) is the period, a is the amplitude; 5 days is the horizontal phase shift chosen. Figure 6b depicts the temperature approximations for the Mwea region.

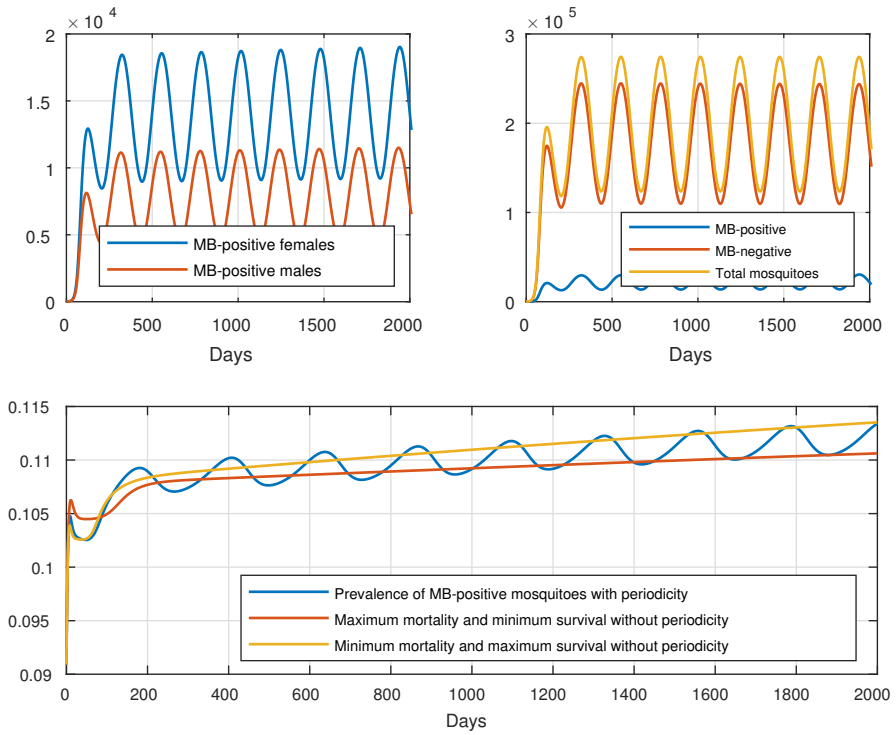

Figure 7. Illustration of the effect of the temperature on the evolution of the population of *MB*-infected mosquitoes. The values of the parameters are: $\beta_h^{mf} = \beta_h^{fm} = 0.35$; $\beta_v = 0.75$; $p_m = 0.7665$; $\epsilon_1 = 1$; $\epsilon_2 = 1$; $t_m = 3$; $n_e = 1$, $K = 200,000$. The remaining parameters d_f, d_m, s and t_e are represented by temperature-dependent functions given in 6b. The first graph describes the population of *MB*-infected females versus the population of *MB*-infected males. The second graph described the total population of *MB*-positive, *MB*-negative mosquitoes and the total population of mosquitoes. The third graph shows the seasonal evolution of the variation of the prevalence of *MB*-infected mosquitoes. In addition, we represented the prevalence given by the autonomous model for the minimum male mortality, minimum female mortality and maximum survival and then for the maximum male mortality, maximum female mortality and minimum survival.

We choose the amplitude $a = 2$ and simulate the model to observe the dynamics of the periodic model. The simulations are presented in Figure 7. From Figure 7, the prevalence of *MB*-infected mosquitoes obtained from the autonomous model for minimum survival and maximum mortality (female and male), as well as the prevalence of *MB*-infected mosquitoes for maximum survival and minimum mortality, could give an approximation of the dynamics of the periodic model at the equilibrium. However, this is not clear enough. As a result, we intend to investigate analytically in further studies how the seasonal dynamics affect the spread of *MB*-infected mosquitoes. Another limitation of this work, from the mathematical point of view is the simple theoretical analysis. Then, a thorough analysis could give more insights into the dynamics of the spread of *MB*-infected mosquitoes. Fur-

thermore, due to the recent discovery of the possibility of utilizing *Microsporidia* MB as a bio-based agent against malaria, there is still a lot to explore mathematically such as the spatial dynamics of *MB*-infected mosquitoes using partial differential equations and the introduction of noises using stochastic models. Finally, we intend to design in further studies, optimal release strategies to increase the prevalence of MB-infected mosquitoes for malaria control, as done in previous dengue-*Wolbachia*-related studies [41, 42].

Use of AI tools declaration

The authors declare they have not used Artificial Intelligence (AI) tools in the creation of this article.

Acknowledgments

The present study was executed by the International Centre of Insect Physiology and Ecology as part of the Symbiont Modeling and Deployment Strategies project, made possible by the generous support of the Bill and Melinda Gates Foundation (INV-022584). Any opinions, findings, conclusions, or recommendations expressed in this publication are those of the authors and do not necessarily reflect the view of the donor. The authors are grateful to the Symbio-vector team of *icipe* for insights on the biological aspect of the symbiont. Author Contributions: Conceptualization: Henri Tonnang, Charlene N. T. Mfangnia, Jeremy Herren, and Berge Tsanou - Mathematical analysis and simulations: Charlene N. T. Mfangnia and Berge Tsanou - Original draft preparation: Charlene N. T. Mfangnia - Writing and review: Charlene N. T. Mfangnia, Henri Tonnang, Berge Tsanou, Jeremy Herren. All authors have read and agreed to the published version of the manuscript.

Conflict of interest

The authors declare there is no conflict of interest.

Availability of data and materials

All data generated or analysed during this study are included in this published article.

References

1. T. G. Andreadis, Microsporidian parasites of mosquitoes, *J. Am. Mosq. Control Assoc.*, **23** (2007), 3–29. https://doi.org/10.2987/8756-971X(2007)23[3:MPOM]2.0.CO;2
2. C. Franzen, Microsporidia: A review of 150 years of research, *Open Parasitol. J.*, **2** (2008), 1–34. https://doi.org/10.2174/1874421400802010001
3. G. Nattoh, T. Maina, E. Makhulu, L. Mbaisi, E. Mararo, G. Fidel, et al., Horizontal transmission of the symbiont microsporidia MB in anopheles arabiensis, *Front. Microbiol.*, **12** (2021). https://doi.org/10.3389/fmicb.2021.647183

4. J. Herren, L. Mbaisi, E. Mararo, E. Makhulu, V. Mobegi, H. Butungi, et al., A microsporidian impairs plasmodium falciparum transmission in anopheles arabiensis mosquitoes, *Nat. Commun.*, **11** (2020), 2187. https://doi.org/10.1038/s41467-020-16121-y
5. J. Akorli, E. A. Akorli, S. N. A. Tetteh, G. K. Amlalo, M. Opoku, R. Pwalia, et al., Microsporidia MB is found predominantly associated with Anopheles gambiae s.s and Anopheles coluzzii in Ghana, *Sci. Rep.*, **11** (2021), 1–5. https://doi.org/10.1038/s41598-021-98268-2
6. K. Haag, J. F. Pombert, Y. Sun, N. De Albuquerque, B. Batliner, P. Fields, et al., Microsporidia with vertical transmission were likely shaped by nonadaptive processes, *Genome Biol. Evol.*, **12** (2020), 3599–3614. https://doi.org/10.1093/gbe/evz270
7. E. Gill, J. Becnel, N. Fast, Ests from the microsporidian, *BMC Genomics*, **9** (2008), 296. https://doi.org/10.1186/1471-2164-9-296
8. G. Zilio, *Co-evolution between Mosquitoes and Microsporidian Transmission Strategies*, PhD thesis, Université de Neuchâtel, Faculté des Sciences, 2018.
9. B. Zheng, X. Liu, M. Tang, Z. Xi, J. Yu, Use of age-stage structural models to seek optimal wolbachia-infected male mosquito releases for mosquito-borne disease control, *J. Theor. Biol.*, **472** (2019), 95–109. https://doi.org/10.1016/j.jtbi.2019.04.010
10. M. Lipsitch, M. A. Nowak, D. Ebert, R. M. May, The population dynamics of vertically and horizontally transmitted parasites, *Proc. R. Soc. London, Ser. B: Biol. Sci.*, **260** (1995), 321–327. https://doi.org/10.1098/rspb.1995.0099
11. M. Z. Ndii, R. I. Hickson, G. N. Mercer, Modelling the introduction of wolbachia into aedes aegypti mosquitoes to reduce dengue transmission, *ANZIAM J.*, **53** (2012), 213–227. https://doi.org/10.1017/S1446181112000132
12. J. Koiller, M. Da Silva, M. Souza, C. Codeço, A. Iggidr, G. Sallet, *Aedes, Wolbachia and Dengue*, PhD thesis, Inria Nancy-Grand Est (Villers-lès-Nancy, France), 2014.
13. Y. Li, X. Liu, Modeling and control of mosquito-borne diseases with wolbachia and insecticides, *Theor. Popul Biol.*, **132** (2020), 82–91. https://doi.org/10.1016/j.tpb.2019.12.007
14. L. Hu, M. Huang, M. Tang, J. Yu, B. Zheng, Wolbachia spread dynamics in stochastic environments, *Theor. Popul Biol.*, **106** (2015), 32–44. https://doi.org/10.1016/j.tpb.2015.09.003
15. D. E. Campo-Duarte, O. Vasilieva, D. Cardona-Salgado, M. Svinin, Optimal control approach for establishing wmelpop wolbachia infection among wild aedes aegypti populations, *J. Math. Biol.*, **76** (2018), 1907–1950. https://doi.org/10.1007/s00285-018-1213-2
16. Y. Li, X. Liu, A sex-structured model with birth pulse and release strategy for the spread of wolbachia in mosquito population, *J. Theor. Biol.*, **448** (2018), 53–65. https://doi.org/10.1016/j.jtbi.2018.04.001
17. L. Hu, M. Huang, M. Tang, J. Yu, B. Zheng, Wolbachia spread dynamics in multi-regimes of environmental conditions, *J. Theor. Biol.*, **462** (2018), 247–258. https://doi.org/10.1016/j.jtbi.2018.11.009

18. P. A. Ryan, A. P. Turley, G. Wilson, T. P. Hurst, K. Retzki, J. Brown-Kenyon, et al., Establishment of wMel Wolbachia in Aedes aegypti mosquitoes and reduction of local dengue transmission in Cairns and surrounding locations in northern Queensland, Australia, *Gates Open Res.*, **3** (2020), 1547.

19. S. Andreychuk, L. Yakob, Mathematical modelling to assess the feasibility of wolbachia in malaria vector biocontrol, *J. Theor. Biol.*, **542** (2022), 111110. https://doi.org/10.1016/j.jtbi.2022.111110

20. M. Altinli, F. Gunay, B. Alten, M. Weill, M. Sicard, Wolbachia diversity and cytoplasmic incompatibility patterns in Culex pipiens populations in Turkey, *Parasites Vectors*, **11** (2018), 198. https://doi.org/10.1186/s13071-018-2777-9

21. O. Koutou, B. Traoré, B. Sangaré, Mathematical modeling of malaria transmission global dynamics: taking into account the immature stages of the vectors, *Adv. Differ. Equations*, **2018** (2018), 220. https://doi.org/10.1186/s13662-018-1671-2

22. F. A. Dahalan, T. S. Churcher, N. Windbichler, M. K. N. Lawniczak, The male mosquito contribution towards malaria transmission: mating influences the Anopheles female midgut transcriptome and increases female susceptibility to human malaria parasites, *PLoS Pathog.*, **15** (2019), 1–19. https://doi.org/10.1371/journal.ppat.1008063

23. R. Baeshen, Swarming behavior in Anopheles gambiae (sensu lato): current knowledge and future outlook, *J. Med. Entomol.*, **59** (2021), 56–66. https://doi.org/10.1093/jme/tjab157

24. W. Takken, C. Costantini, G. Dolo, A. Hassanali, N. Sagnon, E. Osir, *Mosquito Mating Behaviour*, in *Bridging Laboratory and Field Research for Genetic Control of Disease Vectors*, **11** (2006), 183–188.

25. F. Tripet, T. Thiemann, G. C. Lanzaro, Effect of seminal fluids in mating Between M and S forms of Anopheles gambiae, *J. Med. Entomol.*, **42** (2005), 596–603. https://doi.org/10.1093/jmedent/42.4.596

26. C. L. Lyons, M. Coetzee, S. L. Chown, Stable and fluctuating temperature effects on the development rate and survival of two malaria vectors, anopheles arabiensis and anopheles funestus, *Parasites Vectors*, **6** (2013), 104. https://doi.org/10.1186/1756-3305-6-104

27. Y. Afrane, G. Zhou, B. Lawson, A. Githeko, G. Yan, Life-table analysis of anopheles arabiensis in western kenya highlands: effects of land covers on larval and adult survivorship, *Am. J. Trop. Med. Hyg.*, **77** (2007), 660–666. https://doi.org/10.4269/ajtmh.2007.77.660

28. C. Oliva, M. Benedict, G. Lemperiere, J. Gilles, Laboratory selection for an accelerated mosquito sexual development rate, *Malar. J.*, **10** (2011), 135. https://doi.org/10.1186/1475-2875-10-135

29. R. Maharaj, Life table characteristics of Anopheles arabiensis (Diptera: Culicidae) under simulated seasonal conditions, *J. Med. Entomol.*, **40** (2003), 737–742. https://doi.org/10.1603/0022-2585-40.6.737

30. P. van den Driessche, J. Watmough, Reproduction numbers and sub-threshold endemic equilibria for compartmental models of disease transmission, *Math. Biosci.*, **180** (2002), 29–48, https://doi.org/10.1016/S0025-5564(02)00108-6

31. M. A. Lewis, Z. Shuai, P. van den Driessche, A general theory for target reproduction numbers with applications to ecology and epidemiology, *J. Math. Biol.*, **78** (2019), 2317–2339. https://doi.org/10.1007/s00285-019-01345-4
32. H. R. Thieme, Local stability in epidemic models for heterogeneous populations, in *Mathematics in Biology and Medicine*, Springer, (1985), 185–189. https://doi.org/10.1007/978-3-642-93287-8_26
33. J. C. Kamgang, G. Sallet, Computation of threshold conditions for epidemiological models and global stability of the disease-free equilibrium (DFE), *Math. Biosci.*, **213** (2008), 1–12. https://doi.org/10.1016/j.mbs.2008.02.005
34. H. W. Hethcote, H. R. Thieme, Stability of the endemic equilibrium in epidemic models with subpopulations, *Math. Biosci.*, **75** (1985), 205–227. https://doi.org/10.1016/0025-5564(85)90038-0
35. C. Tadmon, S. Foko, A transmission dynamics model of COVID-19: Case of Cameroon, *Infect. Dis. Modell.*, **7** (2022), 211–249. https://doi.org/10.1016/j.idm.2022.05.002
36. S. Lamichhane, Y. Chen, Global asymptotic stability of a compartmental model for a pandemic, *J. Egypt. Math. Soc.*, **23** (2015), 251–255. https://doi.org/10.1016/j.joems.2014.04.001
37. J. D. Meiss, *Differential Dynamical Systems*, SIAM, 2007.
38. R. M. Okara, M. E. Sinka, N. Minakawa, C. M. Mbogo, S. I. Hay, R. W. Snow, Distribution of the main malaria vectors in kenya, *Malar. J.*, **9** (2010), 69. https://doi.org/10.1186/1475-2875-9-69
39. C. Antonio-Nkondjio, F. Simard, Highlights on anopheles nili and anopheles moucheti, malaria vectors in Africa, in *Anopheles Mosquitoes: New Insights into Malaria Vectors*, InTech, Rijeka (HR), 2013.
40. G. Chandra, D. Mukherjee, Chapter 35 - Effect of climate change on mosquito population and changing pattern of some diseases transmitted by them, in *Advances in Animal Experimentation and Modeling*, Academic Press, (2022), 455–460. https://doi.org/10.1016/B978-0-323-90583-1.00030-1 .
41. B. Zheng, L. Chen, Q. Sun, Analyzing the control of dengue by releasing wolbachia-infected male mosquitoes through a delay differential equation model, *Math. Biosci. Eng.*, **16** (2019), 5531–5550. https://doi.org/10.3934/mbe.2019275
42. D. Cardona-Salgado, D. E. Campo-Duarte, L. S. Sepulveda-Salcedo, O. Vasilieva, M. Svinin, Optimal release programs for dengue prevention using Aedes aegypti mosquitoes transinfected with wMel or wMelPop Wolbachia strains, *Math. Biosci. Eng.*, **18** (2021), 2952–2990. https://doi.org/10.3934/mbe.2021149

AIMS Press